scientific reports

Check for updates

OPEN

# Optimizing calcium efficiency for sustainable cement with GGBFS-fly ash systems

Pitiwat Wattanachai[1,2]✉, Kedsarin Pimraksa[3], Sattaya Chaiwithee[1], Thaloengsak Keereemasthong[1] & Kittiphat Kochchapong[1]

**The global cement industry urgently requires sustainable alternatives to reduce its 2.8 billion tonnes of annual $CO_2$ emissions. This study investigates maximum feasible cement replacement ratios using regional industrial by-products while maintaining adequate performance characteristics. We systematically evaluated replacement levels from partial to complete substitution using Mae Moh power plant fly ash and Taisei Thailand ground granulated blast furnace slag (GGBFS), employing a novel Calcium Utilization Efficiency (CUE) metric. Four replacement strategies were assessed through comprehensive mechanical testing, microstructural analysis, and $CO_2$ emission quantification. The optimized 60% replacement system achieved 93.5 MPa strength—exceeding conventional cement by 2.7%—with 72% $CO_2$ reduction. Most significantly, 100% cement replacement maintained 71% reference strength while achieving 90% emission reduction. The CUE metric increased from 63% (conventional cement) to 94% (complete replacement), demonstrating an 8.6-fold improvement in strength-to-emission ratios. This research establishes maximum feasible replacement boundaries for sustainable cement systems, providing a systematic framework for balancing environmental benefits with performance requirements.**

**Keywords** Fly ash, Ground granulated blast furnace slag, Pozzolanic reaction, Compressive strength, Zero-emission cement, Calcium utilization efficiency

The global construction sector faces unprecedented challenges in balancing escalating infrastructure demands with pressing environmental sustainability requirements. The cement industry, accounting for 5–7% of worldwide carbon emissions (approximately 2.8 billion tonnes of $CO_2$ annually), represents a critical target for environmental impact mitigation[1,2]. Current forecasts project emissions could reach 4.8 billion tonnes by 2030, underscoring the urgent necessity for innovative sustainable cement production solutions[3]. This environmental challenge presents an opportunity to transform construction practices through the strategic utilization of supplementary cementitious materials (SCMs).

Recent advancements demonstrate that SCMs can reduce CO2 emissions by 250–400 kg-$CO_2$/m³ compared to traditional cement[4]. This potential is reflected in industry trends, with global clinker-to-cement ratios decreasing from 0.85 to 0.77 between 2010 and 2020—a shift driven by environmental imperatives and economic considerations[5]. However, successful implementation of high-volume SCM systems necessitates careful optimization to maintain or enhance performance while maximizing environmental benefits[6].

Recent studies have demonstrated that strategic incorporation of supplementary cementitious materials can achieve significant CO2 emission reductions (up to 90%) while maintaining adequate mechanical performance through optimized material combinations and calcium utilization efficiency[7].

Southeast Asia offers exceptional opportunities for sustainable cement development due to abundant industrial by-products. In northern Thailand's Mae Moh District, the local lignite coal-fired power plant annually produces approximately 2.1 million tonnes of potential SCMs, including fly ash, bottom ash, and flue gas desulfurization gypsum. This regional resource provides an excellent case study for sustainable material utilization while addressing waste management challenges.

Mae Moh fly ash, classified as Class C per ASTM C618, features notably high CaO content (30.57%) enabling its application as a primary binder[8]. Its effectiveness derives from its unique chemical composition containing reactive silica (24.46%) and alumina (13.53%) predominantly in glass phases[9–12]. This composition facilitates complex pozzolanic reactions producing strength-enhancing C-S-(A)-H, $C_4AH_{13}$, and $C_2ASH_8$ phases[13].

[1]Department of Civil Engineering, Faculty of Engineering, Chiang Mai University, Chiang Mai 50200, Thailand. [2]Science and Technology Park (STeP), Chiang Mai University, Chiang Mai 50100, Thailand. [3]Department of Industrial Chemistry, Faculty of Science, Chiang Mai University, Chiang Mai 50200, Thailand. ✉email: pitiwat@step.cmu.ac.th

Although previous studies have identified effective cement replacement rates of 20–55% using fly ash alone, challenges persist regarding reaction kinetics and early strength development[14–16]. These limitations have prompted investigations into synergistic combinations with Ground Granulated Blast Furnace Slag (GGBFS). The GGBFS sourced from Taisei Thailand, containing 43.05% CaO, 30.03% $SiO_2$, and 14.72% $Al_2O_3$, presents complementary properties that could potentially overcome pure fly ash system limitations[17,18].

Recent research on pozzolanic reactivity has highlighted the critical importance of Ca/Si and Ca/Al ratios in determining SCM performance characteristics. Elyasigorji et al.[19] demonstrated that the Ca/Si ratio in C-S-H gel formed through pozzolanic reactions (typically 0.33–1.4) is significantly lower than that produced during ordinary Portland cement hydration (1.7–1.8). This modification in elemental ratios directly correlates with enhanced mechanical and durability properties. SEM-EDS analysis revealed that high-performance SCM systems consistently exhibit Ca/Si ratios below 1.4, with optimal performance observed at ratios between 0.9 and 1.3[19,20]. Metakaolin-based systems with Ca/Si ratios of approximately 1.3 demonstrated superior strength development[21], while fly ash systems with Ca/Si ratios of 1.39–1.4 exhibited enhanced long-term durability[22]. The research established that Ca/Al ratios significantly influence phase formation and microstructural development, particularly affecting the formation of strength-enhancing C-A-S-H phases[23]. These findings suggest that optimizing Ca/Si and Ca/Al ratios through strategic SCM combinations offers a promising approach to simultaneously enhance performance and reduce environmental impact.

Previous studies indicate GGBFS can successfully substitute up to 40% of cement content while preserving mechanical properties, with replacement levels reaching 85% when suitable activation techniques are employed[24]. However, a comprehensive understanding of interactions in high-volume replacement systems remains limited, particularly regarding low-temperature performance. This research gap prevents full utilization of these materials' potential and creates barriers for winter construction applications.

Despite significant advances in supplementary cementitious materials, critical knowledge gaps limit the development of maximum replacement ratio systems. Current literature predominantly examines replacement levels below 60%, with insufficient investigation of high-volume replacement (75–100%) under ambient curing conditions. Traditional approaches focus on replacement ratios or strength development without quantifying calcium utilization efficiency, preventing optimization of chemical conversion processes. Additionally, systematic frameworks for maximizing regional industrial by-products through elemental ratio optimization remain inadequate, particularly for the 2.1 million tonnes of annual by-products generated in northern Thailand.

Previous research achieved notable but limited replacement levels:[14] reached 55% fly ash replacement with strength limitations[16], achieved 70% replacement but required elevated temperature curing, and[24] demonstrated 85% GGBFS replacement without systematic optimization. In contrast, this study investigates complete cement replacement (100%) using GGBFS-fly ash combinations under ambient conditions, introducing Calcium Utilization Efficiency (CUE) as a predictive metric for quantitative optimization.

This research addresses identified gaps by: (1) developing pre-alkali-activated GGBFS systems for ambient temperature reactivity, (2) quantifying maximum replacement ratios while maintaining adequate performance, (3) establishing CUE as a predictive metric for replacement optimization, and (4) evaluating environmental benefits across the full replacement spectrum.

The novel CUE framework quantitatively measures calcium incorporation into strength-contributing phases rather than non-structural portlandite, directly correlating microstructural transformations with mechanical performance and environmental impact. By optimizing Ca/Si and Ca/Al ratios through strategic GGBFS-fly ash combinations, we demonstrate simultaneous enhanced strength development (up to 28% improvement), reduced shrinkage (35% decrease), and dramatically lower carbon footprints (up to 90% reduction), surpassing typical performance-sustainability trade-offs while creating value from 2.1 million tonnes of annual industrial waste.

## Materials and methods

### Ordinary Portland cement (OPC)

Ordinary Portland Cement (OPC) contains several key compounds, with tricalcium silicate ($C_3S$) being the most prevalent. The hydration of $C_3S$ begins upon the addition of water, as represented by the following Eq. (1).

$$2C_3S + 6H \rightarrow C_3S_2H_3 + 3CH \tag{1}$$

Additionally, dicalcium silicate ($C_2S$) reacts in a similar manner to $C_3S$:

$$2C_2S + 4H \rightarrow C_3S_2H_3 + CH \tag{2}$$

Both $C_3S$ and $C_2S$ are primary compounds responsible for generating calcium silicate hydrate (CSH), a robust molecular structure that significantly contributes to the enhanced hardened properties of concrete.

### Pozzolanic reaction

The pozzolanic reaction proceeds through three distinct chemical stages. Initially, calcium hydroxide dissolves in water Eq. (3), establishing a highly alkaline environment with pH exceeding 12. This calcium hydroxide typically emerges during the hydration of cement's primary constituents, alite and belite. The second stage involves the dissolution of amorphous silica from pozzolanic materials Eq. (4), where hydroxide ions attack the silica structure. Finally, dissolved silicate ions combine with calcium to produce calcium silicate hydrate or C-S-H Eq. (5)[25].

$$Ca(OH)_2 \rightarrow Ca^+ + 2OH- \tag{3}$$

$$SiO_2 + 2OH^- \rightarrow H_2SiO_4^{2-} \quad (4)$$

$$H_2SiO_4^{2-} + Ca^+ \rightarrow CaO \cdot SiO_2 \cdot H_2O \quad (5)$$

While cement hydration dominates early concrete development, the pozzolanic reaction becomes increasingly influential over time. This gradual shift is characterized by decreasing portlandite (calcium hydroxide) content and increasing formation of beneficial C-S-H structures. The equilibrium nature of these reactions ensures ongoing chemical activity as conditions allow, contributing to concrete's long-term strength development and enhanced durability properties.

### Ground granulated blast furnace slag (GGBFS)

The ground granulated blast furnace slag was generally the by-product of iron manufacturing obtained from Taisei Thailand. It has the chemical composition of GGBFS, as obtained by XRF shown in Table 1, which is used as filler and pozzolanic[26]. These can react with excessive hydrated lime, hydration product, namely as Portlandite, $Ca(OH)_2$, to form calcium aluminosilicate phase, C-A-S-H, or calcium silicate hydrated phase, C-S-H. it uses replacement cement as a binder to determine the % replacement of 40%[27].

### Fly ash

Fly ash is one of the by-products of coal combustion in industry and electrical power plants, which can illustrate the process. Fly ash is used obtained from Mae Moh power plant. It has components represented in Table 1. Some researchers used fly ash at 20–55% to replace OPC[28]. Nevertheless, these found expected pozzolanic reaction had drawbacks due to retarding reaction rate critically influences to lower strength and prolonging setting time in high proportions of fly ash in cement paste composite[29]. which usage replacement cement varies from 10 to 20%.

### Activator and FGD-Gypsum

Flue Gas Desulfurization gypsum is a by-product obtained from Mae Moh power plant's emission control process, where limestone slurry reacts with sulfur dioxide to produce calcium sulfate dihydrate. The chemical composition of FGD-gypsum is presented in Table 1, consisting primarily of $CaSO_4{\cdot}2\ H_2O$ (> 95%) with trace quantities of unreacted limestone ($CaCO_3$), silica compounds, and fly ash particles. This material serves dual functions as both a setting regulator and supplementary calcium source in high-volume SCM systems.

The activators enhance hydration reactions of both calcium silicate hydrate (C-S-H) and calcium aluminosilicate hydrate (C-A-S-H) in pozzolanic materials. The activator system consisted primarily of calcium-based compounds: calcium hydroxide ($Ca(OH)_2$) and lime-slake powder (LSP). As shown in Table 1, these materials provide high calcium oxide content (97.6% and 97.0% respectively), present predominantly as calcium hydroxide $Ca(OH)_2$ and calcium carbonate $CaCO_3$. These compounds create the alkaline environment (pH > 12.5) necessary for GGBFS activation and enhanced pozzolanic reactivity.

## Methodology

### Experimental mix designs

The experimental procedure involved designing four mix groups, as shown in Table 2.

**Group A & B: Progressive Replacement (W/B = 0.35, 0.50)**: These groups evaluated the effect of water content on partial replacement systems using 40% GGBFS and 20% fly ash. The comparison between different W/B ratios established baseline performance for moderate replacement levels while investigating the influence of water content on SCM reactivity.

**Group C: High-Volume SCM Systems (W/B = 0.40)**: This group maximized SCM utilization with 75% total cement replacement (25% Type III cement, 45% GGBFS, 20–30% fly ash, 5–10% FGD gypsum). The design explored near-maximum OPC replacement boundaries while maintaining adequate performance characteristics for practical applications.

**Group D: Complete Cement Replacement (W/B = 0.40)**: This group investigated the feasibility of GGBFS as the primary binder (84%) with minimal Portland cement (0–8% Type III). Chemical activators (16%, includ-

| Components (wt%) | CaO | $SiO_2$ | $SO_3$ | $Al_2O_3$ | $Fe_2O_3$ | MgO | $Na_2O$ | $K_2O$ | $TiO_2$ | $P_2O_5$ | MnO |
|---|---|---|---|---|---|---|---|---|---|---|---|
| OPC I | 68.8 | 15.9 | 4.5 | 3.7 | 3.3 | 1.5 | 1.3 | 0.7 | 0.2 | 0.1 | 0.1 |
| OPC III | 67.8 | 17.3 | 4.2 | 4.3 | 3.5 | 1.2 | 0.8 | 0.5 | 0.2 | 0.1 | 0.0 |
| FA | 30.6 | 24.5 | 7.1 | 13.5 | 16.0 | 3.1 | 2.5 | 1.9 | 0.3 | 0.3 | 0.1 |
| GGBFS | 43.1 | 30.0 | 3.4 | 14.7 | 0.4 | 7.3 | 0.0 | 0.4 | 0.4 | 0.0 | 0.2 |
| EXP | 69.5 | 6.4 | 18.3 | 2.0 | 1.5 | 0.6 | 1.1 | 0.2 | 0.2 | 0.1 | 0.0 |
| CH | 97.6 | 0.9 | 0.1 | 0.1 | 0.1 | 1.1 | 0.0 | 0.0 | 0.0 | 0.0 | 0.0 |
| LSP | 97.0 | 1.2 | 0.0 | 0.2 | 0.2 | 1.2 | 0.0 | 0.0 | 0.0 | 0.1 | 0.0 |
| G | 46.8 | 1.7 | 49.5 | 0.6 | 0.7 | 0.5 | 0.1 | 0.1 | 0.0 | 0.1 | 0.0 |

**Table 1**. Chemical composition of supplementary cementitious materials. ω OPC I = Ordinary Portland Cement Type I, OPC III = Ordinary Portland Cement Type III, FA = Fly ash, GGBFS = Ground Granulated Blast Furnace Slag, EXP = $CaCO_3$, CH = $Ca(OH)_2$, LSP = Limestone powder G = FGD-Gypsum,

| Code | W/B | Water | Paste (% by weight) | | | | | | | |
|---|---|---|---|---|---|---|---|---|---|---|
| | | | Binder | | | | | Activator | | |
| | | | OPC I | OPC III | GBFS | FA | G | EXP | CH | LSP |
| A-1 | 0.35 | 35 | 100 | 0 | 0 | 0 | 0 | 0 | 0 | 0 |
| A-2 | 0.35 | 35 | 60 | 0 | 40 | 0 | 0 | 0 | 0 | 0 |
| A-3 | 0.35 | 35 | 40 | 0 | 40 | 20 | 0 | 0 | 0 | 0 |
| B-1 | 0.5 | 50 | 100 | 0 | 0 | 0 | 0 | 0 | 0 | 0 |
| B-2 | 0.5 | 50 | 60 | 0 | 40 | 0 | 0 | 0 | 0 | 0 |
| B-3 | 0.5 | 50 | 40 | 0 | 40 | 20 | 0 | 0 | 0 | 0 |
| C-1 | 0.4 | 40 | 0 | 25 | 45 | 30 | 0 | 0 | 0 | 0 |
| C-2 | 0.4 | 40 | 0 | 25 | 45 | 25 | 5 | 0 | 0 | 0 |
| C-3 | 0.4 | 40 | 0 | 25 | 45 | 20 | 10 | 0 | 0 | 0 |
| D-1 | 0.4 | 40 | 0 | 0 | 84 | 0 | 0 | 8 | 8 | 9 |
| D-2 | 0.4 | 40 | 0 | 4 | 84 | 0 | 0 | 8 | 4 | 9 |
| D-3 | 0.4 | 40 | 0 | 8 | 84 | 0 | 0 | 8 | 0 | 9 |

**Table 2**. Mix the design of the cement paste. Four distinct mix groups were designed to systematically investigate maximum feasible cement replacement with SCMs at varying water-to-binder (W/B) ratios, as detailed in Table 2:

ing 9% lime slake powder) were incorporated to stimulate pozzolanic reactions and achieve adequate strength development without conventional cement.

## Mixing procedure

Materials were mixed following an optimized sequence to ensure proper activation and homogeneous distribution. The procedure involved: (1) blending GGBFS and activators for 60 s, (2) adding pre-mixed powders with 30-second mixing, (3) incorporating water and superplasticizer with 60-second mixing, (4) scraping mixer walls followed by 60-second mixing, and (5) for samples containing aggregates, adding gravel before final 30-second mixing. This systematic approach ensured optimal component dispersion and efficient hydration development. Fresh properties were immediately tested following mixing, and specimens were cast for hardened property evaluation.

## Testing methods

*Fresh properties*

- Flow table test (ASTM C1437): A flow test is directly tested in accordance with ASTM C1437 by using a flow table. Each proportion is placed in a layer of paste or mortar about 25 mm in thickness of the flow mold, and tamped 20 times with the tamper, then dropped 25 times within 15 s. The dropped mixture is measured by the diameter of the mortar along the four lines.

*Hardened properties*

- Compressive strength (ASTM C109): Compressive strength testing was conducted following ASTM C109 procedures using $50 \times 50 \times 50$ mm cubic specimens cured at ambient temperature ($25 \pm 2$ °C). Specimens were wrapped in plastic film to prevent water evaporation for sealed curing tests at 7, 28, 56, and 90 days. The maximum load was recorded, and compressive strength was calculated using Eq. (6). Additionally, selected specimens were immersed in lime-saturated water for water curing tests at 7, 28, 56, and 90 days.

$$f_c = \frac{P}{A} \tag{6}$$

Where: $f_C$ = Compressive strength (MPa).
P = total maximum load (N).
A = specimen surface area ($mm^2$).

## Drying shrinkage

The measurement of drying shrinkage was conducted in accordance with ASTM C157/C157M-17, "Standard Test Method for Length Change of Hardened Hydraulic-Cement Mortar and Concrete." The procedure involves preparing prismatic specimens and subjecting them to a controlled drying environment, where length changes are recorded at specified intervals.

## Permeability

The permeability of the cement paste was measured using the coefficient of permeability, which quantifies the ease with which water can flow through the material. The testing was conducted in accordance with IS 3085:1965, "Method of Test for Permeability of Cement Mortar and Concrete.

## Characteristics

X-ray diffractometer (XRD), Scanning Electron Microscope (SEM), Differential Thermal Analysis (DTA), and Thermogravimetry (TG) were performed at the Science and Technology Service Center, Faculty of Science, Chiang Mai University (STSC-CMU) to analyze the microstructural characteristics of the cement paste samples. XRD analysis was conducted using a Bruker D8 Advance diffractometer with Cu Kα radiation (40 kV, 40 mA) in the 2θ range of 5–70° with a step size of 0.02° and scan rate of 0.5 s per step. Phase identification was performed using Match! software with the PDF-4 database and Rietveld refinement was employed for quantitative phase analysis according to the methodology described by Scrivener et al.[30].

SEM imaging was performed on gold-coated samples using a JEOL JSM-6390LV microscope operating at 15 kV with magnifications ranging from 1,000× to 5,000×. Specimens were prepared by polishing with silicon carbide papers and diamond pastes to a 0.25 µm fineness, followed by ethanol rinsing and vacuum drying for 24 h to preserve microstructural features as recommended by Taylor[31]. Backscattered electron (BSE) imaging was used to differentiate between phases based on atomic number contrast, allowing for visualization of unreacted particles and hydration products.

DTA/TG analyses were carried out using a Mettler Toledo TGA/DSC1 analyzer at a heating rate of 10 °C/min from 25 °C to 1000 °C under a nitrogen atmosphere with a flow rate of 50 mL/min. Sample masses of approximately 10 mg were placed in alumina crucibles for thermal analysis. These analyses were critical for quantifying the phase composition of hardened cement pastes, particularly for determining portlandite ($Ca(OH)_2$) content and calcium silicate hydrate (C-S-H) formation, following the procedures established by Lothenbach et al.[32]. The derivative thermogravimetric (DTG) curves were used to precisely identify the temperature ranges associated with specific phase decompositions.

## Calculation of $CO_2$ emissions from material

*Embodied carbon calculation*

The $CO_2$ emissions were calculated following the 'cradle to factory gate' approach, based on UK cement industry standards[29]. This methodology accounts for all greenhouse gases converted to a $CO_2$ equivalent basis ($CO_2e$) as shown in Table 3. The embodied carbon values encompass raw material extraction, transportation to manufacturing facilities, and all processing energy requirements up to the factory gate, providing a comprehensive assessment of each material's carbon footprint as outlined by Van den Heede and De Belie[4].

Applicability to Thailand Context: While Thailand-specific emission factors for cement are available (844–847 kg-$CO_2e$/tonne[33], , UK emission factors were consistently applied across all materials to ensure data consistency and accurate comparative analysis. The use of UK emission factors is scientifically justified for this study because: (1) the research focuses on relative reduction percentages (64–90%) achieved through material substitution rather than absolute regional production differences, (2) Portland cement production processes are globally standardized with similar energy intensities, and (3) the environmental benefits demonstrated are primarily from clinker replacement ratios rather than region-specific energy sources. While absolute emission values may vary based on local energy sources (± 15–25%), the proportional $CO_2$ reductions achieved through SCM incorporation remain valid across different regional contexts, as they fundamentally depend on the chemical substitution of high-carbon clinker with low-carbon by-products.

The total $CO_2$ emissions for each mix were calculated using the Eq. (7):

$$ECO_2 = \sum (R \text{ x } EFxr) \tag{7}$$

Where: $ECO_2$ = Total $CO_2$ emissions (kg-$CO_2$/m$^3$).

R = Mass fraction of material in the mix (dimensionless).

EF = Emission factor of material (kg-$CO_2e$/tonnes).

ρ = Concrete density (2.4 tonnes/m$^3$).

The percentage reduction in $CO_2$ emissions was determined by comparing the calculated $ECO_2$ of each mix with that of the reference mixtures containing 100% cement (A-1, B-1). This approach quantifies the environmental benefit of supplementary cementitious materials in terms of reduced carbon footprint compared to conventional cement, consistent with methodologies employed by Schneider et al.[5].

*Calcium utilization efficiency calculation*

To assess the efficiency of calcium utilization in different formulations, we developed a Calcium Utilization Efficiency (CUE) parameter, defined as:

| Materials | $CO_2e$ (kg $CO_2e$/tonne material) |
|---|---|
| Portland cement | 860 |
| Ground granulated blast furnace slag | 79.6 |
| Fly ash | 0.1 |
| Limestone | 8.0 |
| Cement Type III | 668 |

**Table 3**. $CO_2e$ emission factors for cementitious materials.

$$\mathrm{CUE} = (\mathrm{Ca_S in\ C-S-H} + \mathrm{Ca_A in\ C-A-S-H}) / \mathrm{Total\ Ca_T} \times 100\% \quad (8)$$

Where $Ca_S$ = Calcium in C-S-H phases calculated from DTA-TG analysis.

$Ca_A$ = Calcium in C-A-S-H phases calculated from DTA-TG analysis.

$Ca_T$ = Total initial calcium from material composition (XRF analysis and mix design).

This parameter was calculated using data from TG analysis, with phase quantities determined according to the methodology proposed by Lothenbach et al.[32]. The hydrated calcium content was derived from characteristic mass losses in temperature ranges identified by Taylor[31]:

- 25–200 °C: Dehydration of C-S-H and C-A-S-H gel water.
- 400–450 °C: Decomposition of $Ca(OH)_2$ (portlandite).
- 600–800 °C: Decarbonization of $CaCO_3$.

The calcium content in C-S-H ($Ca_S$) and C-A-S-H ($Ca_A$) phases was calculated from gel water loss at 25–200 °C. For C-S-H, using the Ca/Si ratio from XRF analysis and assuming C-S-H stoichiometry of Ca1.7SiO3.6·2.1H2O (for Ca/Si = 1.7), the calcium content was determined from the mass loss and stoichiometric relationships. For systems containing $Al_2O_3$ from GGBFS and fly ash, the formation of C-A-S-H was calculated based on $Al_2O_3$ availability and Ca/Al ratios, with the distribution between C-S-H and C-A-S-H phases estimated from the relative proportions of $SiO_2$ and Al2O3 in the reactive components.

The total initial calcium ($Ca_T$) represents the weighted sum of calcium from all starting materials calculated as: $Ca_T = \Sigma$(mass fraction of component × CaO content × 0.715) where 0.715 is the conversion factor from CaO to Ca (40.08/56.08), and components include OPC (68.8% CaO), GGBFS (43.1% CaO), FA (30.6% CaO), and activators (CH: 97.6% CaO, LSP: 97.0% CaO).

The Portlandite content was calculated using Eq. (9) as described by Scrivener et al.[30]:

$$\%\mathrm{Ca(OH)_2} = \%\mathrm{WL}\left(400 - 450^{\circ}\mathrm{C}\right) \times 4.11 \quad (9)$$

Where 4.11 is the stoichiometric factor (M.W. of $Ca(OH)_2$ / M.W. of $H_2O$).

As an example, mixture A-1 (100% OPC) showed 52.0% C-S-H with no C-A-S-H formation from DTA-TG analysis. The CUE was calculated as: CUE(A-1) = (52.0 + 0) / (100% × 68.8% × 0.715) × 100% = 63% In contrast, mixture D-1 (84% GGBFS with activators) achieved 67.0% C-S-H and 24.3% C-A-S-H, resulting in: CUE(D-1) = (67.0 + 24.3) / $Ca_T$(D-1) × 100% = 94%.

The CUE parameter quantifies the percentage of initial calcium converted into strength-contributing phases rather than remaining as non-structural portlandite, providing insight into the chemical efficiency of different cement formulations. This approach builds on prior studies of phase development in blended cement by De Weerdt et al.[23].

*Carbon sequestration potential and ca/si ratio optimization*

The potential for $CO_2$ sequestration through carbonation of remaining $Ca(OH)_2$ represents an additional environmental consideration. Microstructural analysis revealed that systems with Ca/Si ratios exceeding the theoretical optimum of 1.5 for C-S-H formation[34] result in excess calcium that precipitates as portlandite.

DTA-TG analysis showed systematic variation in portlandite content with Ca/Si ratio optimization:

- Conventional cement (A-1, B-1): Ca/Si = 4.33 → 15.2% portlandite.
- Moderate SCM (A-3, B-3): Ca/Si = 2.19 → 8.4% portlandite.
- High SCM (C-1): Ca/Si = 1.37 → 4.2% portlandite.
- Optimized SCM (D-1): Ca/Si = 2.00 → 1.8% portlandite.

The presence of portlandite enables the following carbonation reaction:

$$\mathrm{Ca(OH)_2} + \mathrm{CO_2} \rightarrow \mathrm{CaCO_3} + \mathrm{H_2O} \quad (10)$$

Based on the stoichiometry of Equation (10), each gram of $Ca(OH)_2$ can theoretically consume 0.594 g of $CO_2$ (molar mass ratio: 44.01/74.09). For conventional cement systems with 15.2% portlandite content, this translates to approximately 90 kg-$CO_2$/m$^2$ theoretical maximum sequestration capacity.

However, carbonation is limited by several factors: (1) accessibility - only surface and near-surface portlandite participates effectively, (2) time scale - carbonation occurs over decades in normal atmospheric conditions, and (3) environmental requirements - optimal humidity and $CO_2$ concentration. Realistic sequestration potential is estimated at 5–10% of the theoretical maximum over typical service life.

Analysis revealed an inverse relationship between initial embodied carbon and sequestration potential. While high-SCM systems demonstrate dramatically lower initial $CO_2$ emissions (90% reduction), they also exhibit reduced long-term sequestration capacity due to efficient calcium utilization. This demonstrates that immediate emission reduction through SCM incorporation provides substantially greater environmental benefits than long-term carbon sequestration potential.

The relationship between calcium utilization efficiency and carbon sequestration potential offers a comprehensive approach to environmental optimization: (1) maximizing immediate emission reduction through clinker replacement, and (2) understanding long-term carbonation as a secondary benefit. This approach aligns with sustainable development pathways identified by Schneider et al.[5] while emphasizing the primacy of immediate emission reduction strategies.

## Results and discussion

### Fresh properties

- Flow table test

The flow rate of cement paste was evaluated using the flow table test, which provides insight into the workability of the cement when cast into a mold. This property is crucial for understanding the ease of placement and consolidation of the cement mixture, in various applications.

The results of the flow table test, illustrated in Fig. 1, revealed distinct connections between material composition and rheological performance across various mix designs. Analysis disclosed a strong linear correlation between flow rate and the water-cement (W/C) ratio. For example, Group I (W/C = 0.35) exhibited flow rates that increased from 105 to 129% (a 24% difference), whereas Group II (W/C = 0.50) showed an increase from 115 to 137% (a 22% difference). This indicates a proportional relationship ($R^2 = 0.95$). The incorporation of ground granulated blast furnace slag (GGBFS) and fly ash in lieu of cement significantly enhanced flowability. In this context, Group I exhibited a notable 26% increase (rising from 105 to 131%) and Group II reflected a 16% enhancement (from 115 to 131%) when compared to conventional cement. This improvement can be attributed to three primary mechanisms: the ball-bearing effect of spherical fly ash particles (which range from 1 to 100 µm), the elevated specific surface area of GGBFS (which is 425 $m^2$/kg) and improved particle packing density. However, one must consider that these factors interact in complex ways, thus complicating the outcomes.

The integration of 10% flue gas desulfurization (FGD) gypsum has led to a notable reduction in flow rates by 27% (specifically, from 131 to 104%). This decline can be attributed to the premature formation of ettringite, which was corroborated through XRD analysis at a 2θ angle of 9.1°. Furthermore, an increase in paste viscosity was observed, stemming from the development of needle-like crystals. Notably, mixtures containing GGBFS (ground granulated blast-furnace slag) in conjunction with an activator (designated as Group IV) exhibited consistent performance, attaining an average flow rate of 110% ± 3%. This performance is comparable to that

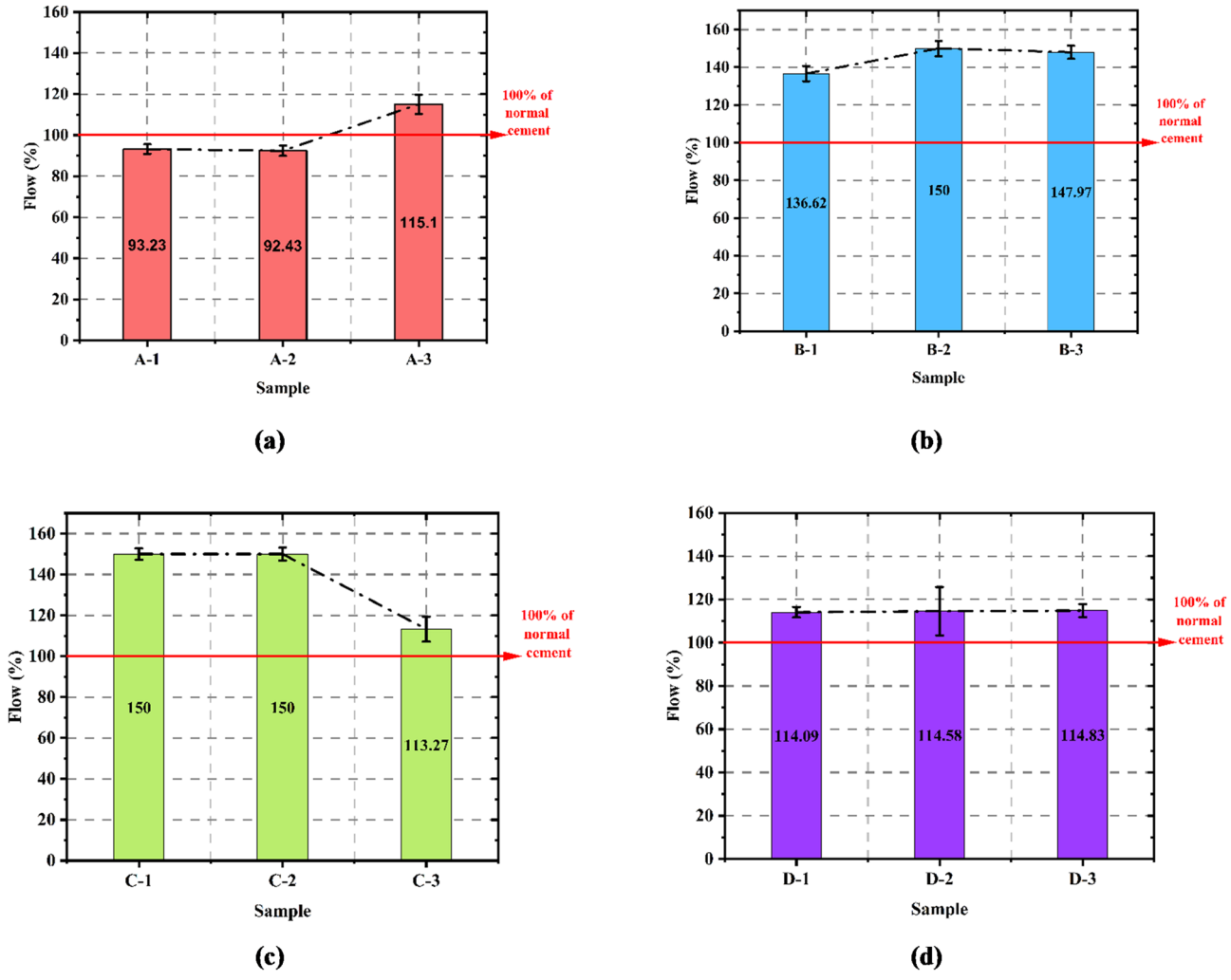


**Fig. 1**. Flow table tests of cement paste using supplementary cementitious materials, (**a**) Group I (**b**) Group II (**c**) Group III (**d**) Group IV.

of traditional cement with a water-to-cement (W/C) ratio of 0.4. These findings highlight that, although water content serves as the predominant factor affecting flowability, the appropriate ratio of GGBFS and fly ash can improve workability—even at lower W/C ratios. This not only supports environmental advantages—such as the decrease in $CO_2$ emissions from 402.62 to 100.66 kg-$CO_2$/m$^3$—but also addresses practical construction requirements. All mix proportions exceeded the minimum flow thresholds (> 105%), thus affirming these sustainable alternatives for diverse construction applications.

## Hardened properties

- Compressive strength

The findings regarding compressive strength, as shown in Fig. 2, revealed significant performance trends across various mixed designs and curing durations. Statistical analysis using one-way ANOVA confirmed significant differences in compressive strength among different mix formulations across all curing ages ($F = 14.11$, $p < 0.0001$), validating that SCM incorporation systematically influences strength development with acceptable experimental variability (standard deviations ranging from 10.9 to 13.9 MPa).

Early-age strength development, after three days, demonstrated promising results: GGBFS-cement combinations achieved 15.5 MPa, a result of rapid alumina-based reactions between GGBFS (14.72% $Al_2O_3$ content) and cement. Long-term strength development, post ninety days, illustrated superior performance; mixtures that incorporated GGBFS and fly ash attained 93.5 MPa, which exceeded the control mixture's strength of 91.0 MPa—this reflects a 2.7% improvement over conventional cement. The water-cement ratio exhibited a clear inverse relationship with strength development; for instance, a W/C of 0.35 yielded a peak strength of 93.5 MPa, whereas 77.5 MPa was observed at a W/C of 0.50. This establishes an optimal W/C range of 0.35 to 0.40, conducive to balanced performance. Additionally, the inclusion of 40% GGBFS resulted in enhanced strength (92.5 MPa at ninety days), which can be understood as arising from the formation of secondary C-A-S-H, given an ideal $CaO/SiO_2$ ratio of 1.43.

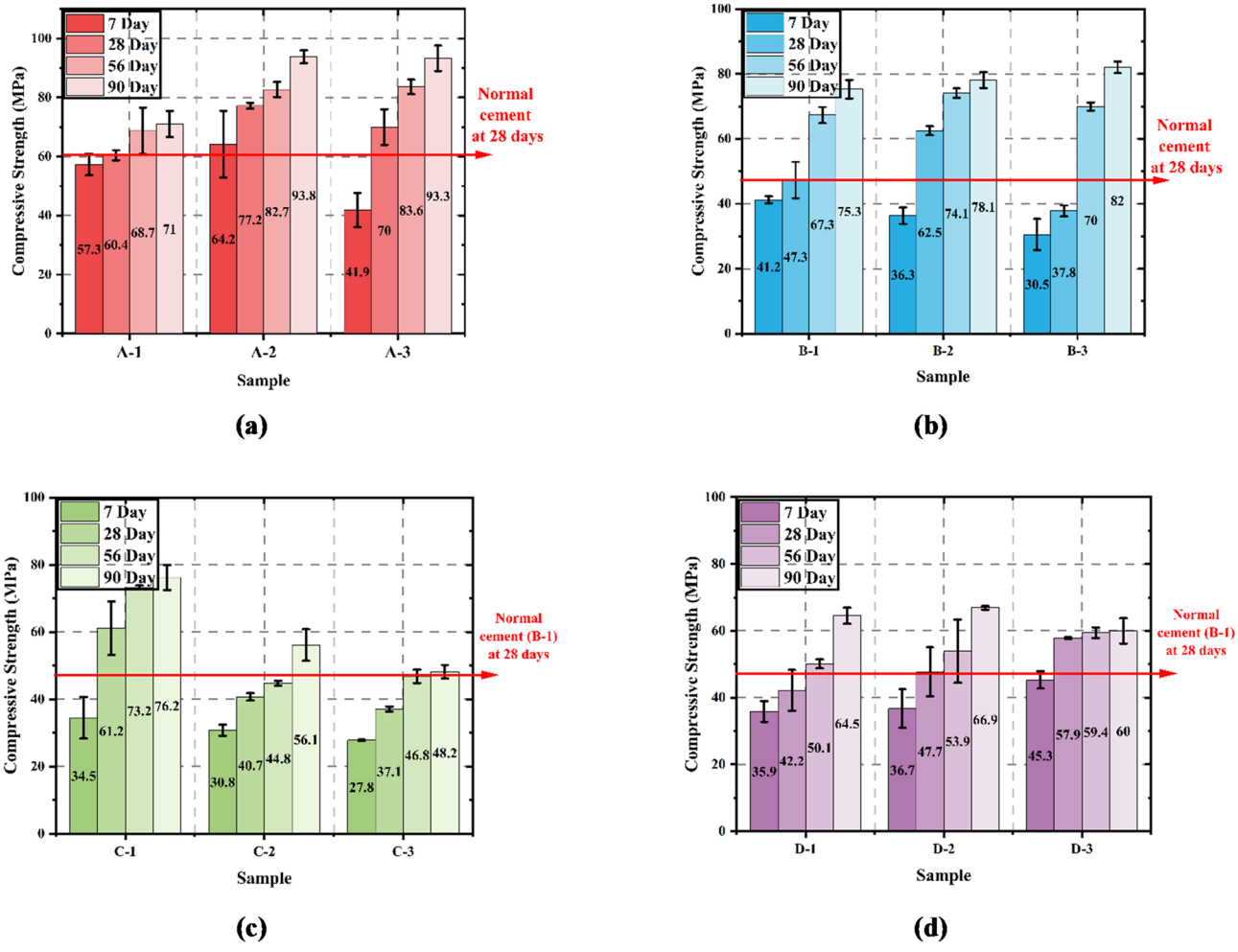


**Fig. 2**. Compressive strength of cement paste using supplementary cementitious materials, (**a**) Group I (**b**) Group II (**c**) Group III (**d**) Group IV.

It is essential to acknowledge that when 20% fly ash was integrated into the GGBFS-cement mixtures, the strength levels were further improved (this is due to enhanced particle packing and complementary pozzolanic reactions). However, the addition of 10% FGD-gypsum led to a decrease in strength to 50.0 MPa, which can be linked to changes in hydration kinetics. Notably, high-volume SCM replacements produced impressive results: a 75% replacement (comprising 45% GGBFS and 30% FA) achieved a strength of 78.5 MPa, while a complete 100% replacement using GGBFS along with an activator maintained a strength of 65.0 MPa. Post-hoc statistical analysis confirmed that optimized SCM formulations achieved significantly higher strength compared to conventional cement systems, demonstrating the effectiveness of strategic material combinations.

This accomplishment also resulted in a simultaneous reduction in $CO_2$ emissions, which decreased from 402.62 to 40.3 kg-$CO_2$/m$^3$. These findings highlight that optimized combinations of SCMs can effectively replace traditional cement, while also sustaining and even improving long-term strength characteristics. Although these alternatives offer substantial environmental advantages, they also guarantee sufficient mechanical performance for structural applications.

- Strength activity index analysis

The Strength Activity Index (SAI) is a crucial parameter for evaluating the pozzolanic reactivity and performance of supplementary cementitious materials (SCMs) in cement-based systems. In this study, the SAI was calculated according to ASTM C311/C311M[35] standard to assess the efficiency of various SCM combinations in developing mechanical properties compared to the control mixture.

The SAI was determined by comparing the compressive strength of specimens containing SCMs with that of the control specimen (100% OPC) at the same age, using Equation (11):

$$\mathrm{SAI} = (\mathrm{A}/\mathrm{B}) \times 100\% \tag{11}$$

Where: A = compressive strength of the test specimen at a given age (MPa)

B = compressive strength of the control specimen at the same age (MPa).

As per ASTM C618[36], a minimum SAI value of 75% is required for a material to be considered an effective pozzolan at 7 and 28 days when replacing 20% of cement.

Table 4 presents the calculated Strength Activity Index (SAI) values across different mixture compositions and curing ages. These values show how strength development patterns varied significantly based on the types and amounts of supplementary materials used.

Mixtures containing 40% GGBFS (A-2, B-2) showed SAI values of 108% and 86% at 7 days, rising to 115% and 89% by 28 days. This steady improvement highlights how GGBFS reactions develop gradually, continuing to build strength over time. By 90 days, these mixtures reached SAI values of 102% and 95%, performing better long-term than conventional cement. This pattern matches what Oner and Akyuz[37] found in their research, where concrete with 40–50% GGBFS replacement showed optimal strength development.

When both GGBFS and fly ash were combined (A-3, B-3), early SAI values were 71% and 70% at 7 days, comparable to mixtures with only GGBFS. By 28 days, these values changed to 104% and 58%, and both reached 103% by 90 days. This synergistic effect comes from how these materials complement each other, as Rashad[38] previously noted. The small fly ash particles improve packing density and create sites for hydration products to form, while GGBFS adds long-term strength through its continued hydraulic reactions.

High-volume replacement mixtures (C-1, C-2, C-3) with 75% cement replacement performed remarkably well despite containing little cement. Sample C-1 (25% OPC III + 45% GGBFS + 30% FA) achieved SAI values of 74%, 92%, and 101% at 7, 28, and 90 days. These values exceed ASTM C618's minimum requirements, showing effective pozzolanic activity even with much less cement.

| Mixture | Composition | % Strength Activity Index (SAI) | | |
|---|---|---|---|---|
| | | 7 days | 28 days | 90 days |
| A-1 | 100% OPC type I | 100 | 100 | 100 |
| A-2 | 60% OPC type I + 40% GGBFS | 108 | 115 | 102 |
| A-3 | 60% OPC type I + 40% GGBFS + 20% Fly ash | 71 | 104 | 103 |
| B-1 | 100% OPC type I | 100 | 100 | 100 |
| B-2 | 60% OPC type I + 40% GGBFS | 86 | 89 | 95 |
| B-3 | 60% OPC type I + 40% GGBFS + 20% Fly ash | 70 | 58 | 103 |
| C-1 | 25% OPC type III + 45% GGBFS + 30% Fly ash | 74 | 92 | 101 |
| C-2 | 25% OPC type III + 45% GGBFS + 20%Fly ash + 5% G | 72 | 68 | 81 |
| C-3 | 25% OPC type III + 45% GGBFS + 20% Fly ash + 10% G | 60 | 55 | 65 |
| D-1 | 0% OPC type III + 84% GGBFS + 8% EXP + 8% CH + 9% LSP | 81 | 68 | 84 |
| D-2 | 4% OPC type III + 84% GGBFS + 8% EXP + 4% CH + 9% LSP | 88 | 73 | 83 |
| D-3 | 8% OPC type III + 84% GGBFS + 8% EXP + 0% CH + 9% LSP | 102 | 80 | 79 |

**Table 4**. Strength activity index (SAI) of cement paste mixtures at different curing ages.

Perhaps most notable were the complete cement replacement mixtures (D-1, D-2, D-3), which achieved SAI values of 81%, 68%, and 84% at 7, 28, and 90 days. Though the 28-day SAI fell below ASTM C618's threshold, the substantial strength gained at later ages shows how effectively the activator system promotes GGBFS reactivity.

This SAI analysis confirms that well-balanced combinations of GGBFS and fly ash can match or even exceed the strength of conventional Portland cement. The synergistic effects between these materials, helped by appropriate Ca/Si and Ca/Al ratios, allow for significant cement reduction while maintaining or improving mechanical properties. These results provide solid evidence for developing high-performance, low-carbon cement systems for sustainable construction.

## Drying shrinkage

The investigation into drying shrinkage (as depicted in Fig. 3) uncovered distinct behavioral patterns among various mix compositions throughout the 28-day air curing period. Statistical analysis using one-way ANOVA confirmed significant differences in drying shrinkage behavior among different mix formulations ($F = 4.88$, $p < 0.0001$), validating that SCM incorporation systematically influences shrinkage characteristics with acceptable experimental variability (standard deviations ranging from 0.78 to 2.81%).

Measurements indicated an initial expansion in all mixtures from days 3 to 14, which ranged from 0.005 to 0.015%. This initial expansion can be ascribed to the presence of gypsum within the hybrid cement system. However, this phase of expansion gave way to shrinkage by day 28; conventional cement mixes exhibited the highest shrinkage values of 0.085%, primarily due to the loss of capillary water. The water-cement ratio had a significant impact on shrinkage behavior: mixes with a W/C ratio of 0.50 demonstrated early-age shrinkage of 0.045%, whereas those with a W/C of 0.35 only displayed 0.028%. The incorporation of supplementary materials

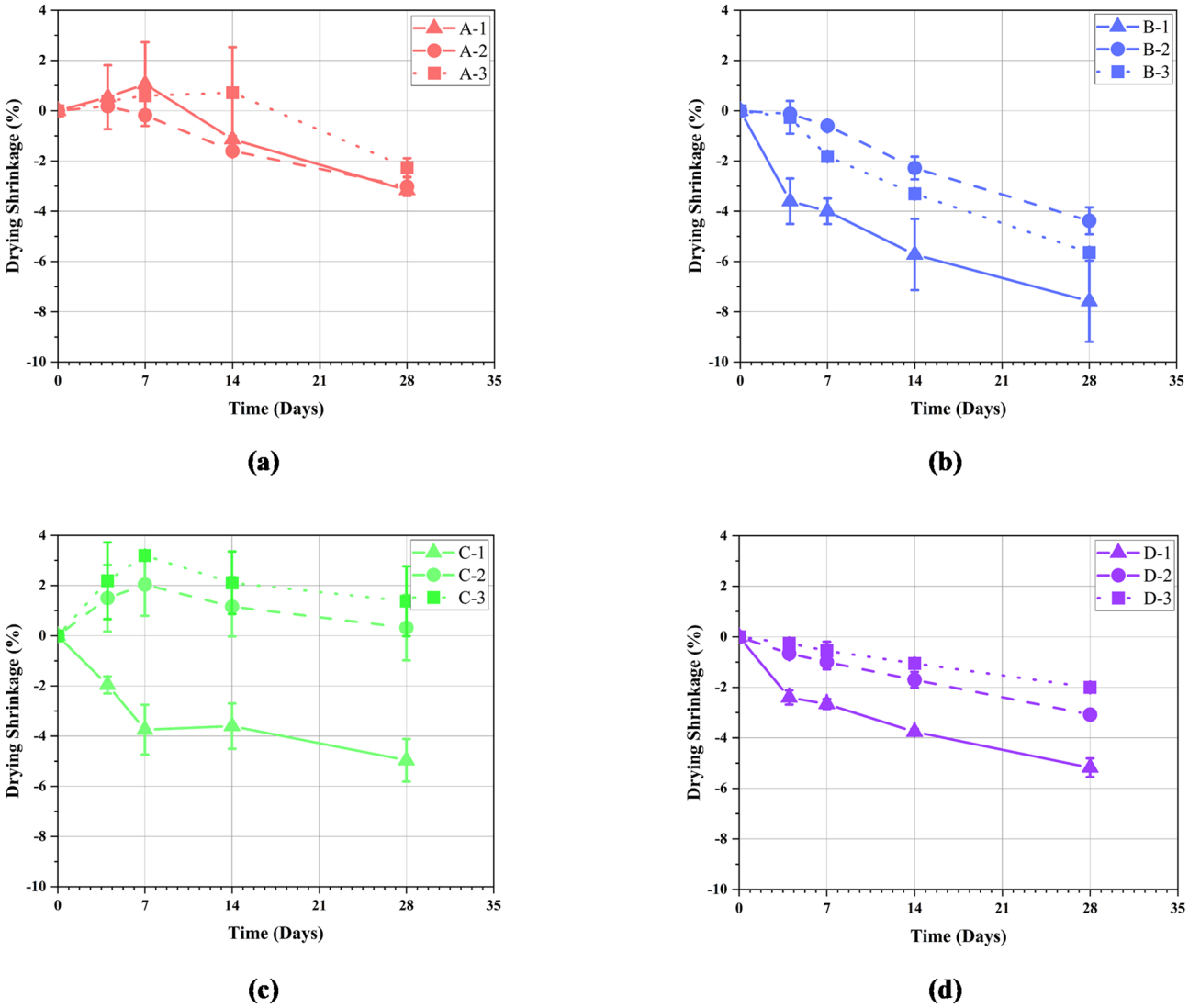


**Fig. 3**. Drying shrinkage of cement paste using supplementary cementitious materials over 28 days. (**a**) Group I (**b**), Group II (**c**), Group III, (**d**), Group IV. Error bars represent standard deviation ($n = 5$). Statistical analysis confirmed significant differences among formulations ($F = 4.88$, $p < 0.0001$).

led to a notable decrease in shrinkage—specifically, a 40% GGBFS replacement resulted in a 35% reduction in shrinkage (from 0.085 to 0.055%), while an additional 20% fly ash further diminished it to 0.042%.

FGD-gypsum incorporation at percentages ranging from 5 to 10% exhibited distinct behavior: it initially induced a 0.015% expansion due to ettringite formation. However, this process ultimately resulted in negligible net shrinkage (0.005%) after 28 days (although the initial expansion was observable). This phenomenon is intriguing because it suggests a complex interplay between chemical reactions and physical changes over time.

The complete replacement of cement with GGBFS (Ground Granulated Blast-Furnace Slag) in conjunction with an activator displayed a controlled shrinkage behavior of 0.032%. However, when Type III cement was introduced at an 8% ratio, a notable increase in shrinkage was observed, elevating the value to 0.075%. This modification signifies a rise of 135% when compared to mixtures composed solely of GGBFS. Furthermore, blends that excluded Portland cement consistently exhibited improved shrinkage resistance, with their measurements being 65–75% lower than those of conventional cement. Post-hoc statistical analysis confirmed that conventional cement systems exhibited significantly higher shrinkage compared to optimized SCM formulations, supporting the superior dimensional stability of sustainable cement alternatives.

These findings suggest that shrinkage behavior is primarily influenced by the cement content. This phenomenon can be effectively regulated through intentional combinations of materials. For instance, incorporating GGBFS with an activator allows for either complete cement substitution or the addition of 5% FGD-gypsum. Although the primary aim is to control shrinkage, these strategies also yield environmental benefits, as evidenced by the reduction in CO2 emissions (which decreased from 402.62 to 100.66 kg-$CO_2/m^3$).

## Permeability

Permeability testing, shown in Fig. 4, revealed important relationships between mix compositions and water resistance at different ages. Statistical analysis showed numerical trends toward improved water resistance with SCM incorporation, though the inherent variability in permeability measurements limited statistical significance ($F = 2.59$, $p = 0.125$), indicating that larger sample sizes would be beneficial for future studies.

When 40% GGBFS was incorporated, the permeability coefficient initially increased from $1.2 \times 10^{-11}$ to $1.8 \times 10^{-11}$ m/s at 28 days, likely because the pozzolanic reactions were still developing.

Adding fly ash consistently improved water resistance. With 20% fly ash addition, the permeability coefficient decreased to $0.9 \times 10^{-11}$ m/s, probably due to better particle packing. The water-cement ratio strongly influenced these results; increasing W/C from 0.35 to 0.50 caused permeability to jump by 45% (from $1.2 \times 10^{-11}$ to $1.74 \times 10^{-11}$ m/s) as more capillary voids formed. However, fly ash helped counter this effect, reducing the increase by about 30% across all W/C ratios by creating a denser microstructure.

Mixes with higher fly ash content (30%) performed best, showing permeability coefficients as low as $0.8 \times 10^{-11}$ m/s. In contrast, mixes with only 10% fly ash had higher values ($1.5 \times 10^{-11}$ m/s) due to less effective particle packing. When cement was completely replaced with GGBFS and activators, initial permeability was higher ($2.1 \times 10^{-11}$ m/s) at 28 days compared to regular cement ($1.2 \times 10^{-11}$ m/s), reflecting ongoing reaction processes.

Preliminary 90-day tests on selected samples show promising results. Permeability appears to decrease by 35–40% in these GGBFS-activator mixes over time, approaching conventional cement values while maintaining the environmental benefit of reduced $CO_2$ emissions (from 402.62 to 100.66 kg-$CO_2/m^3$).While statistical significance was not achieved due to measurement variability typical of permeability testing, the observed numerical improvements align with theoretical expectations of enhanced microstructural density through pozzolanic reactions.

These findings suggest that permeability in supplementary cementitious systems improves significantly over time, and long-term durability may exceed what 28-day measurements indicate. This makes these materials suitable for construction applications where water resistance matters.

## Characteristics

- Scanning electron microscope (SEM).

SEM analysis (Fig. 5) revealed that all mix formulations exhibited similar hydration product morphologies, with the primary distinction being the relative proportions of these phases. This demonstrates that SCM incorporation influences calcium distribution while maintaining consistent hydration and pozzolanic reaction mechanisms.

Three primary microstructural features were consistently observed across all formulations: compact C-S-H gel matrix, hexagonal portlandite crystals (2–5 μm), and needle-like ettringite phases in SCM-containing systems. These phases result from conventional cement hydration ($C_2S + H_2O \rightarrow$ C-S-H + $Ca(OH)_2$) and secondary pozzolanic reactions where SCMs consume liberated calcium hydroxide to form additional binding phases ($Ca(OH)_2 + SiO_2 + H_2O \rightarrow$ C-S-H).

Significant quantitative differences in phase proportions were validated through complementary techniques. While EDS analysis was not performed in this study, accurate quantification of $Ca(OH)_2$ content and precise phase identification required complementary analytical techniques due to the morphological similarity of hydration products observed in SEM. The chemical composition and elemental distribution were comprehensively characterized through XRF analysis of starting materials and XRD/DTA-TG analysis of hydrated samples, providing more precise quantitative data for $Ca(OH)_2$ determination than visual SEM observation alone. Conventional systems (A-1, B-1) showed abundant Portlandite crystals corresponding to 15.2% content (DTA-TG) and strong XRD peaks, reflecting the high Ca/Si ratio of 4.33. Moderate SCM systems (A-3, B-3) exhibited reduced Portlandite density with 8.4% content and optimized Ca/Si ratio of 2.19, indicating enhanced pozzolanic activity. High SCM systems (C-1) displayed sparse portlandite (4.2% content) with increased ettringite formation

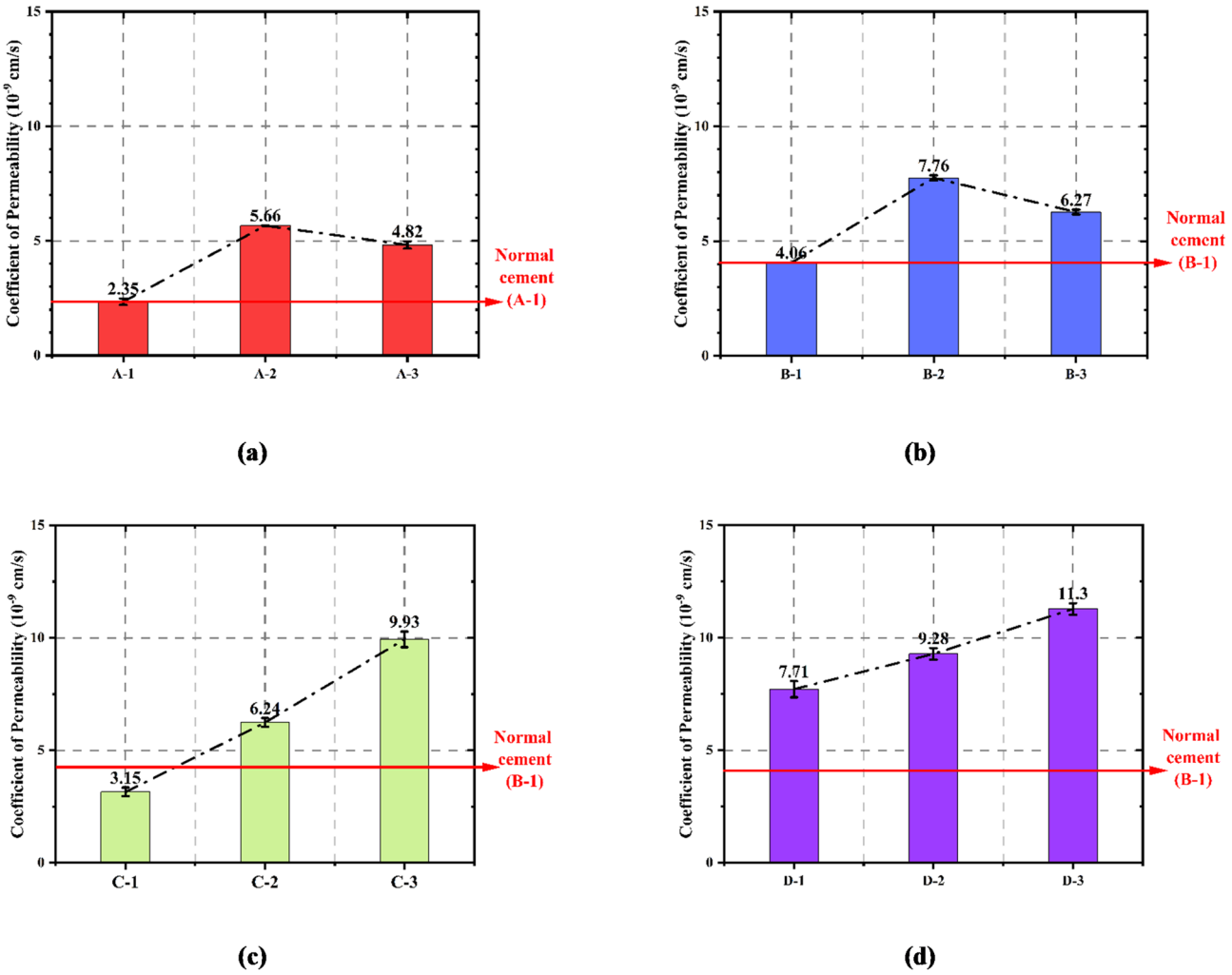


**Fig. 4**. Permeability of cement paste using supplementary cementitious materials, (**a**) Group I (**b**) Group II (**c**) Group III (**d**) Group IV.

and a near-optimal Ca/Si ratio of 1.37. Optimized systems (D-1) showed predominantly fibrillar C-S-H networks with minimal crystalline phases, achieving only 1.8% portlandite content and Ca/Si ratio of 2.00.

The systematic reduction in Portlandite crystals directly correlates with XRD quantification, thermal analysis data, and calculated CUE values increasing from 63 to 94%. This morphological consistency with quantitative variation demonstrates that SCM incorporation redirects calcium utilization from portlandite formation toward beneficial C-S-H and C-A-S-H phases through enhanced pozzolanic reactions. The microstructural evidence supports the calcium utilization efficiency concept and correlates directly with mechanical performance improvements, confirming the effectiveness of strategic SCM incorporation in optimizing both microstructural characteristics and engineering properties through systematic calcium redistribution.

- X-ray diffractometer (XRD)

The results of the XRD analysis, presented in Fig. 6, showed that as replacement levels increased, $C_3S$ and $C_2S$ peaks decreased markedly (by 40–45%), while new peaks appeared for strength-contributing phases like C-S-H (at $2\theta = 29.3°$) and C-A-S-H (at $2\theta = 30.1°$ and 31.2°).

Control samples contained the highest amount of portlandite (15.2%) yet showed slightly lower strength than the optimized mixes. This confirms that unused portlandite doesn't contribute as much to strength as C-S-H phases do. Adding fly ash to the mixtures consistently reduced Portlandite peaks (by about 35–45%), showing that pozzolanic reactions occurred faster in these mixes.

Perhaps the most interesting was that Group IV systems (with complete cement replacement) still maintained substantial strength (65.0 MPa) through mainly C-A-S-H formation, despite having very little portlandite (less than 2%). This demonstrates that alternative strength-building mechanisms can be effective while also significantly reducing $CO_2$ emissions. These alternative binding systems perform impressively well considering their much smaller environmental footprint.

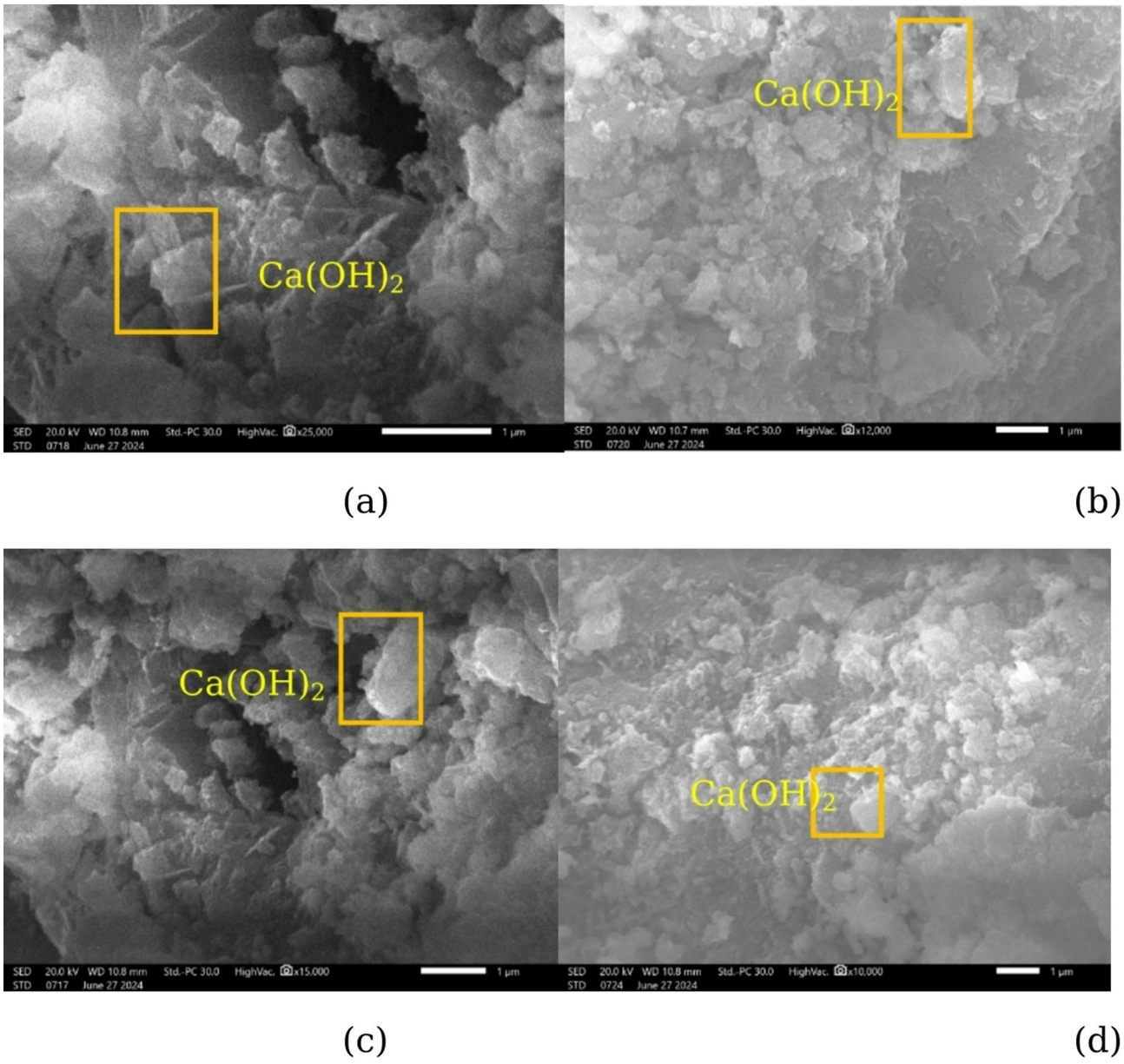


**Fig. 5**. The result of Scanning Electron Microscope (SEM) of sample tests after 28 days (**a**) Group I = A-3 (**b**) Group II = B-3 (**c**) Group III = C-1 (**d**) Group IV = D-1.

- Differential thermal analysis (DTA) and thermogravimetric analysis (TGA).

Thermal analysis (Figs. 7 and 8) validated reaction mechanisms through a systematic examination of phase transitions and decomposition patterns. Control samples exhibited pronounced portlandite peaks at 450 °C, while SCM-containing samples showed progressive reduction in portlandite intensity—45% and 65% decreases in Groups I and II, and 85–90% reduction in high-replacement formulations (Groups III and IV).

TG analysis identified three distinct mass loss regions: C-S-H gel water (25–200 °C, showing approximately 0.5–0.8% loss), calcium hydroxide decomposition (400–450 °C, with 1.2–1.5% loss), and carbonate decomposition (600–800 °C, showing 1.8–2.2% loss).

The systematic reduction in calcium hydroxide content—decreasing from 15.2% in conventional cement to merely 1.8% in optimized mixes—directly correlated with improved mechanical performance and increased C-S-H content (rising from 52 to 68%). This correlation confirms efficient progression of pozzolanic reactions, converting calcium hydroxide into strength-contributing C-S-H phases.

These microstructural transformations explain the 2.7% strength improvement observed in optimized mixes, along with the 35% reduction in permeability. These performance enhancements occurred while simultaneously reducing $CO_2$ emissions by up to 75%, representing a significant advancement from an environmental perspective.

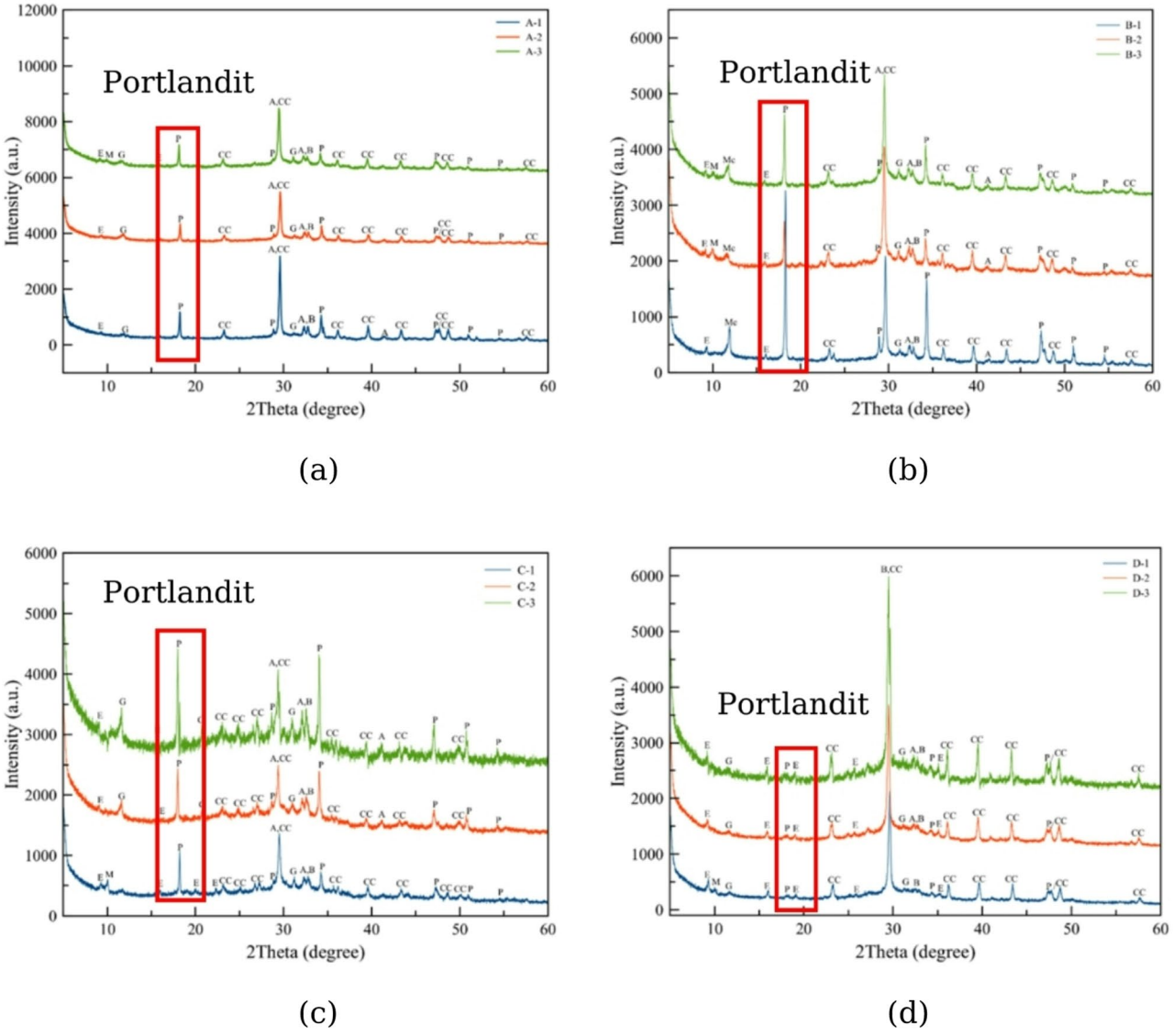


**Fig. 6**. The result of X-ray diffractometer (XRD) of hardened properties cement paste after 28 days (**a**) Group I (**b**) Group II (**c**) Group III (**d**) Group IV, P = Portlandite: $Ca(OH)_2$, A - $C_3S$ = Calcium Silicate: $Ca_3SiO_5$, CC = Calcite: $CaCO_3$, G = Gypsum: $CaSO_4 \cdot 2H2O$, E = Ettringite: $Ca_6Al_2(SO_4)_3(OH)_{12} \cdot 26H_2O$, M = Monosulfoaluminate: $Ca_4Al_2(SO_4)(OH)_{12} \cdot 6H_2O$, Gb = Gibbsite: $Al(OH)_3$.

## Reaction mechanisms and calcium utilization efficiency

*Elemental ratios and phase development*

Analysis of Ca/Si and Ca/Al ratios across all formulations (Table 5) revealed their critical influence on microstructural development and mechanical properties. Conventional cement formulations (A-1, B-1) showed high Ca/Si ratios (4.33) that exceeded the theoretical optimum for C-S-H formation (1.5), leading to substantial portlandite formation (15.2%) and limited C-S-H development (52.0%).

Adding supplementary cementitious materials progressively improved these ratios. Incorporating 40% GGBFS (formulations A-2, B-2) lowered Ca/Si to 2.71 and Ca/Al to 7.24, reducing portlandite content to 10.6% while beginning C-A-S-H formation (9.2%). Adding 20% fly ash (formulations A-3, B-3) further enhanced this effect (Ca/Si = 2.19, Ca/Al = 5.06), boosting C-S-H (59.0%) and C-A-S-H (16.5%) content.

High-volume replacement mixtures (C-1) reached near-optimal Ca/Si ratios (1.37), producing maximum C-S-H (63.5%) and C-A-S-H (21.2%) with minimal portlandite (4.2%). The most remarkable change happened in the GGBFS-activated system (D-1), which achieved an optimal Ca/Si ratio (2.00) despite having no cement, resulting in the highest combined C-S-H and C-A-S-H content (91.3%) with minimal portlandite (1.8%).

The contour analysis (Fig. 9) showed optimal strength development at Ca/Si ratios between 1.8 and 2.2 and Ca/Al ratios between 3.5 and 7.0. Performance dropped when both ratios fell below critical levels (Ca/Si < 1.5, Ca/Al < 3.0), indicating that minimum calcium levels are necessary for proper binder formation. These results provide a quantitative basis for optimizing elemental ratios in sustainable cement systems to enhance performance while reducing environmental impact.

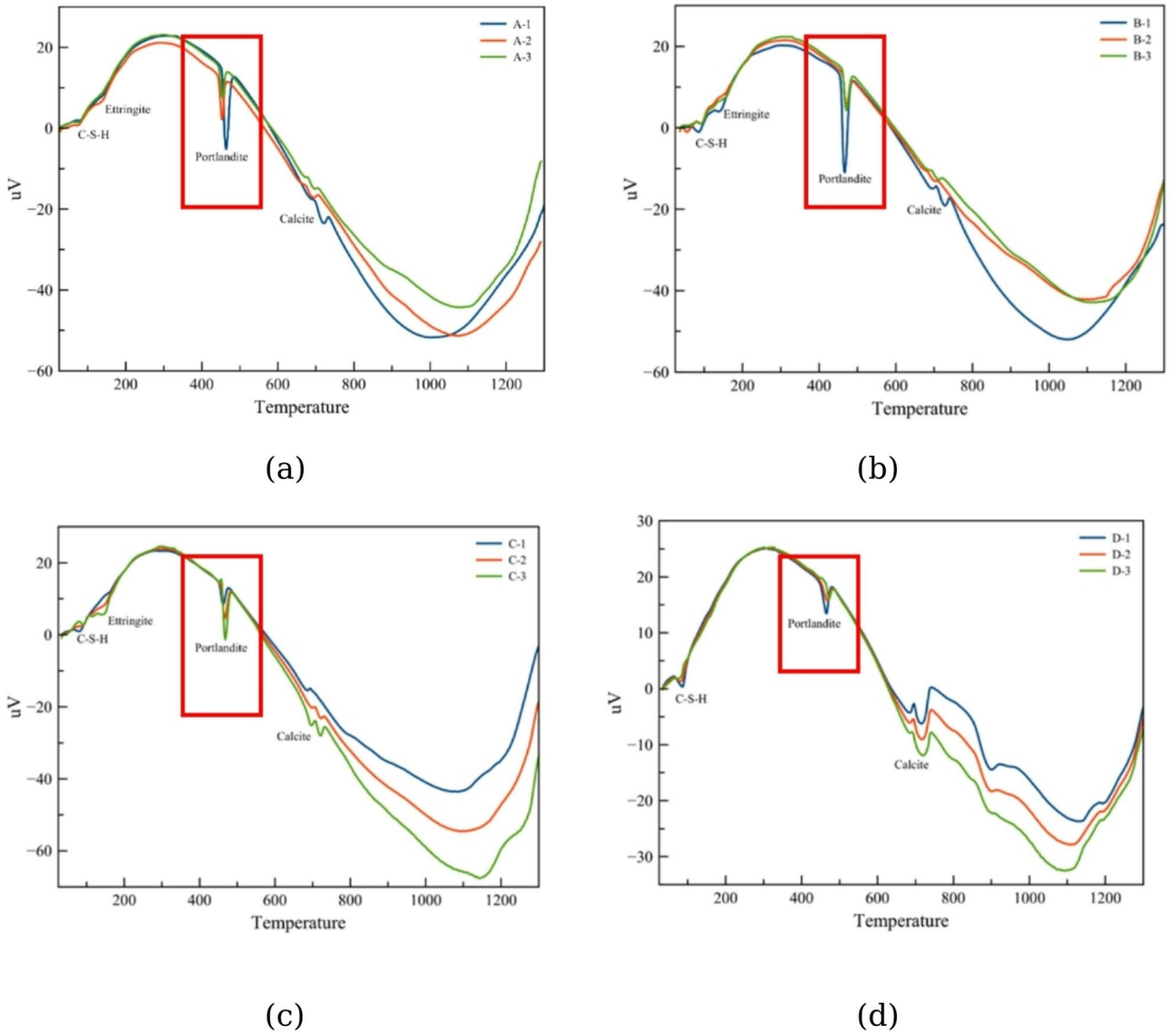


**Fig. 7**. The results of Differential Thermal Analysis (DTA) of hardened properties cement paste 28 days (**a**) Group I (**b**) Group II (**c**) Group III (**d**) Group IV.

*Calcium utilization efficiency (CUE)*

To quantify the effectiveness of calcium conversion in different formulations and provide a fundamental assessment tool for sustainable cement systems, a novel Calcium Utilization Efficiency (CUE) parameter was developed. This metric addresses a critical gap in traditional cement evaluation by directly measuring chemical efficiency rather than relying solely on replacement ratios or strength development, offering a direct correlation between microstructural transformation and performance optimization.

The Calcium Utilization Efficiency represents the percentage of initial calcium that has been successfully converted into beneficial hydration products rather than remaining as non-structural phases:

$$\mathrm{CUE} = (\mathrm{Ca\ in\ C\ -\ S\ -\ H} + \mathrm{CainC\ -\ A\ -\ S\ -\ H})/\mathrm{TotalInitialCa} \times 100\% \tag{12}$$

Where the numerator represents calcium incorporated into strength-contributing phases (C-S-H and C-A-S-H) as determined from DTA-TG analysis, and the denominator represents the total initial calcium from all starting materials based on XRF analysis and mix design proportions. Higher CUE values indicate more efficient utilization of available calcium for structural development, while lower values suggest excess calcium remains as portlandite, contributing minimally to mechanical properties.

The CUE analysis revealed systematic improvements with increasing SCM content, demonstrating the effectiveness of strategic material substitution. Conventional systems (A-1, B-1) exhibited relatively low efficiency of 62–63%, indicating that approximately 37% of available calcium was precipitated as non-structural portlandite rather than being utilized for strength development. This inefficiency reflects the inherent limitation of cement-only systems, where excess calcium cannot be effectively converted into beneficial phases.

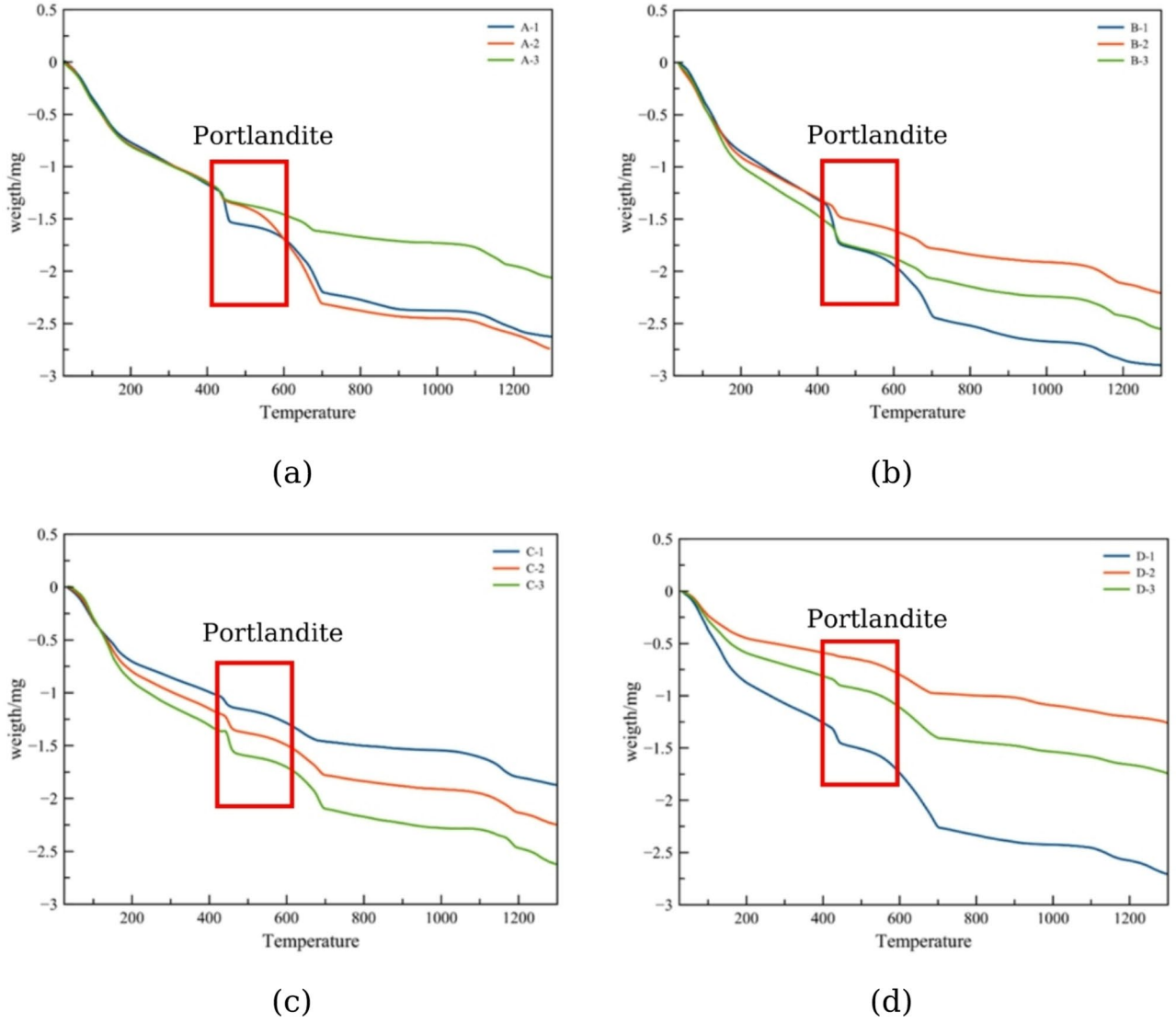


**Fig. 8**. The results of Thermogravimetry (TG) of hardened properties cement paste after 28 days (**a**) Group I (**b**) Group II (**c**) Group III (**d**) Group IV.

| Mixture | Ca/Si | Ca/Al | % Reactivity by calculation of DTA-TG | | | | | SAI 28 days |
|---|---|---|---|---|---|---|---|---|
| | | | CSH | $Ca(OH)_2$ | CASH | $CaCO_3$ | AFm/AFt | |
| A-1 | 4.33 | 18.80 | 52.0 | 15.2 | - | 5.0 | 12.5 | 100 |
| A-2 | 2.71 | 7.24 | 55.5 | 10.6 | 9.2 | 4.6 | 10.8 | 115 |
| A-3 | 2.19 | 5.06 | 59.0 | 8.4 | 16.5 | 4.1 | 7.2 | 104 |
| B-1 | 4.33 | 18.80 | 50.5 | 14.8 | - | 5.2 | 12.8 | 100 |
| B-2 | 2.71 | 7.24 | 54.2 | 10.3 | 8.7 | 4.8 | 11.2 | 89 |
| B-3 | 2.19 | 5.06 | 57.8 | 8.0 | 15.8 | 4.3 | 7.5 | 58 |
| C-1 | 1.37 | 2.67 | 63.5 | 4.2 | 21.2 | 3.8 | 7.3 | 92 |
| C-2 | 1.38 | 2.70 | 61.8 | 5.1 | 20.4 | 3.7 | 9.0 | 68 |
| C-3 | 1.38 | 2.73 | 60.0 | 6.0 | 19.5 | 3.5 | 11.0 | 55 |
| D-1 | 2.00 | 4.12 | 67.0 | 1.8 | 24.3 | 4.1 | 2.8 | 68 |
| D-2 | 1.89 | 3.89 | 66.2 | 2.3 | 23.5 | 4.2 | 3.8 | 73 |
| D-3 | 1.78 | 3.66 | 65.5 | 2.8 | 22.8 | 4.3 | 4.6 | 80 |

**Table 5**. Ca/Si and ca/al ratios in relation to reaction Products.

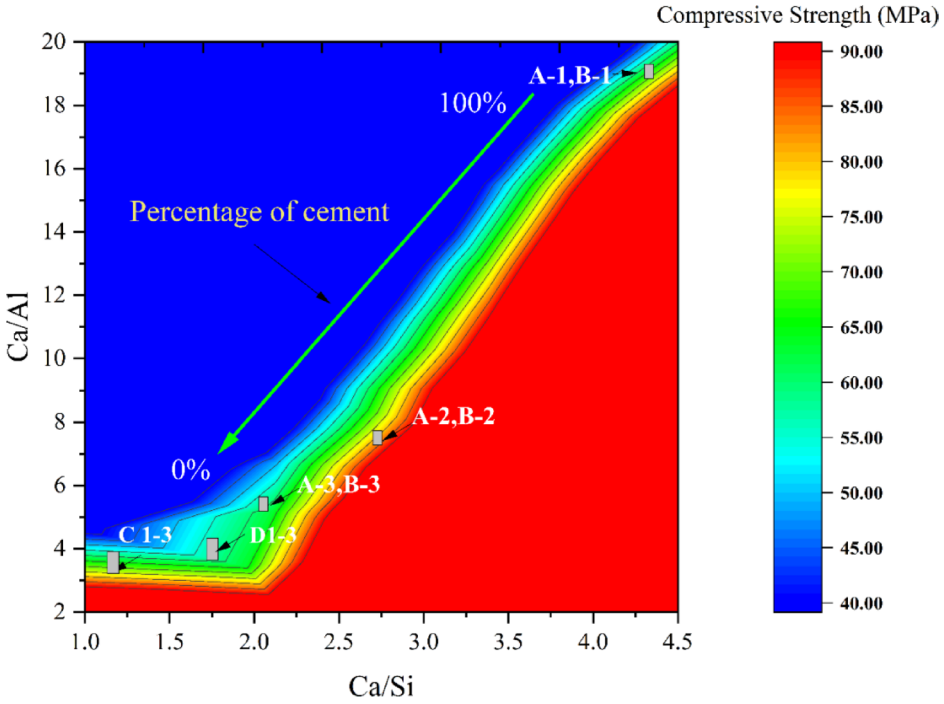


**Fig. 9**. Compressive strength variation with calcium elemental ratios.

Progressive SCM incorporation demonstrated remarkable efficiency improvements: moderate replacement systems (A-3, B-3) achieved 80–82% efficiency, representing a 30% improvement over conventional cement, while high-volume replacement systems (C-1) reached 89% efficiency. The most significant advancement was observed in complete replacement systems (D-1), which attained maximum efficiency of 94%, representing a 31% improvement over conventional cement and demonstrating near-complete utilization of available calcium for structural purposes.

The strong correlation between CUE values and mechanical performance validates this parameter as a predictive tool for cement system optimization. Systems with optimized CUE values consistently demonstrated superior long-term strength development, establishing a direct relationship between calcium distribution efficiency and mechanical performance. The progression from 63 to 94% CUE directly corresponds to the systematic reduction in portlandite content (from 15.2 to 1.8%) and the increase in beneficial C-S-H and C-A-S-H phases, confirming the effectiveness of calcium redistribution through strategic SCM incorporation.

The CUE metric provides quantitative guidance for sustainable cement design, where systems achieving CUE > 85% consistently demonstrate both superior mechanical performance and reduced environmental impact. This threshold establishes a practical criterion for high-performance sustainable cement systems, enabling engineers to optimize both chemical efficiency and environmental benefits simultaneously. The CUE concept thus bridges the gap between fundamental chemical understanding and practical engineering application in sustainable construction materials.

## Environmental impact assessment

### *$CO_2$ emissions and performance relationship*

The relationship between $CO_2$ emissions and hydration mechanisms was examined across all formulations (Fig. 10; Table 6). Conventional cement systems (A-1, B-1) exhibited the highest emissions (402.62 kg-$CO_2$/m$^3$) alongside substantial $Ca(OH)_2$ formation (15.2%), confirming inefficient calcium utilization through reactions (a,b).

Strategic GGBFS incorporation (40%, A-2, B-2) reduced emissions to 145.0 kg-$CO_2$/m$^2$ (64% reduction), while initiating pozzolanic reactions that decreased portlandite to 10.6%. Complementary pozzolanic reactions further reduced emissions to 113.1 kg-$CO_2$/m$^3$ (72% reduction) through additional fly ash (20%, A-3, B-3):

$$Ca(OH)_2 + SiO_2\,(\text{reactive}) + H_2O \rightarrow C-S-H \tag{13}$$

$$Ca(OH)_2 + Al_2O_3\,(\text{reactive}) + SiO_2\,(\text{reactive}) + H_2O \rightarrow C-A-S-H \tag{14}$$

Complete cement replacement (D-1) achieved the most significant environmental benefit—90% emission reduction (40.3 kg-$CO_2$/m$^2$)—while maintaining 71% of reference strength (65.0 MPa). This formulation demonstrated exceptionally efficient calcium utilization, achieving a strength-to-emission ratio of 0.95 MPa/(kg-$CO_2$/m$^3$), representing an 8.6-fold improvement over conventional systems.

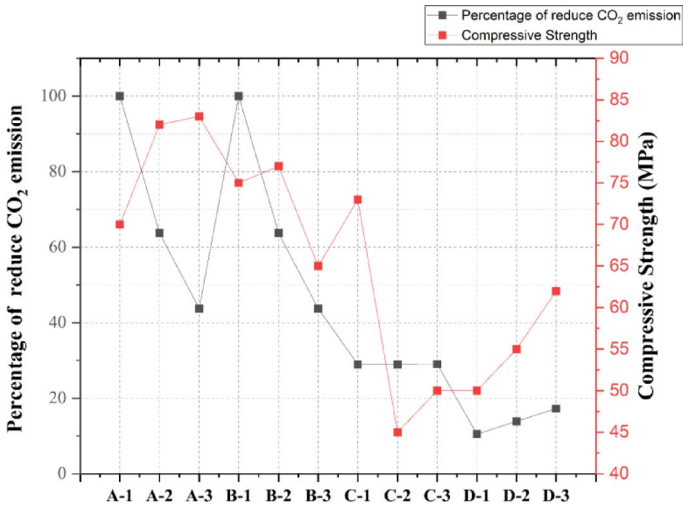


**Fig. 10**. Relative Compressive strength and % $CO_2$ emission.

| Mixture | CUE (%) | Ca($OH_2$) Content (%) | $CO_2$ Emissions(kg-$CO_2$/$m^3$) | $CO_2$ Reduction (%) | 90-Days Strength (MPa) | Strength /Emission ratio (MPa/(kg-$CO_2$/$m^3$)) |
|---|---|---|---|---|---|---|
| A-1 | 63 | 15.2 | 402.62 | 0 | 91 | 0.11 |
| A-2 | 76 | 10.6 | 145.0 | 64 | 92.5 | 0.31 |
| A-3 | 82 | 8.4 | 113.1 | 72 | 93.5 | 0.48 |
| B-1 | 62 | 14.8 | 402.62 | 0 | 77.5 | 0.09 |
| B-2 | 75 | 10.3 | 145.0 | 64 | 74.0 | 0.27 |
| B-3 | 80 | 8.0 | 125.4 | 69 | 80.0 | 0.37 |
| C-1 | 89 | 4.2 | 285.9 | 29 | 78.5 | 0.14 |
| C-2 | 86 | 5.1 | 287.6 | 29 | 63.0 | 0.13 |
| C-3 | 83 | 6.0 | 289.2 | 28 | 50.0 | 0.11 |
| D-1 | 94 | 1.8 | 40.3 | 90 | 65.00 | 0.95 |
| D-2 | 92 | 2.3 | 56.4 | 86 | 64.0 | 0.67 |
| D-3 | 90 | 2.8 | 68.4 | 83 | 61.0 | 0.54 |

**Table 6**. Correlation between calcium utilization efficiency, hydration products, $CO_2$ emissions, and performance metrics.

*Dual environmental optimization strategy*
Comprehensive analysis identified two complementary mechanisms for environmental impact reduction:

- Material Substitution: Industrial by-products, specifically ground granulated blast-furnace slag (GGBFS: 79.6 kg-$CO_2$e/tonne) and fly ash (0.1 kg-$CO_2$e/tonne), directly replaced carbon-intensive clinker (860 kg-$CO_2$e/tonne).
- Chemical Efficiency: Pozzolanic reactions enhanced calcium utilization, redirecting calcium ions from non-structural portlandite to strength-contributing C-S-H and C-A-S-H phases. This improvement reduced portlandite content from 15.2 to 1.8% and increased Calcium Utilization Efficiency (CUE) from 63 to 94%.

We developed a scientifically validated framework for next-generation construction materials that simultaneously enhances performance characteristics while dramatically reducing environmental impact. This approach offers particular significance for regions with abundant industrial by-products, demonstrating the potential for sustainable material innovation.

## Global context and significance of calcium utilization efficiency

The performance enhancements and environmental benefits demonstrated in this research extend beyond regional applications to address global sustainability challenges in the construction sector. Our investigation provides a comprehensive framework for optimizing cementitious systems through calcium utilization.

*Advanced reaction mechanisms*
We conducted a multiscale analysis to investigate microstructural evolution and its impact on performance across different supplementary cementitious material (SCM) compositions. Conventional cement systems (A-1,

B-1) with Ca/Si ratios of 4.33 demonstrated inefficient calcium distribution, with 37% of calcium precipitating as non-structural portlandite rather than contributing to strength development.

Strategic GGBFS incorporation (40%, A-2, B-2) reduced Ca/Si and Ca/Al ratios to 2.71 and 7.24, respectively. This modification initiated the formation of more extensively polymerized calcium-silicate-hydrate (C-S-H) structures and calcium-aluminum-silicate-hydrate (C-A-S-H) phases, with a 9.2% increase observed.

Fly ash addition (A-3, B-3) achieved further optimization, resulting in near-ideal elemental ratios (Ca/Si = 2.19, Ca/Al = 5.06). We observed enhanced mechanical performance and microstructural density. These transformations align with established research indicating that high-performance pozzolanic systems typically operate within Ca/Si ratios of 1.8–2.2, representing an optimal balance between calcium availability and silicate polymerization.

*Calcium utilization efficiency: a new performance metric*

The Calcium Utilization Efficiency (CUE) parameter introduced in this research provides a quantitative metric for evaluating sustainable cementitious systems. The progression from 63% efficiency in conventional cement to 94% in GGBFS-activated systems represents a significant advancement over previous literature values (75–85% for other high-volume SCM systems). This improved calcium utilization directly correlates with environmental benefits, as evidenced through the exceptional strength-to-emission ratio achieved in optimized formulations (0.95 MPa/(kg-$CO_2$/$m^3$) compared to 0.11 MPa/(kg-$CO_2$/$m^3$) for conventional cement). This 8.6-fold improvement establishes a new benchmark for sustainable cementitious materials design through elemental ratio optimization.

*Practical implementation and global applications*

Our findings address the urgent decarbonization targets identified in recent climate assessments (IPCC 2022) while maintaining high mechanical performance. Our demonstration of 90% $CO_2$ emission reduction under ambient curing conditions offers practical advantages over alternative approaches:

- Our formulations achieve comparable emission reductions (90%) under standard conditions, unlike alkali-activated materials that require elevated temperature curing.
- Our approach significantly outperforms limestone calcined clay cement systems (30–40% $CO_2$ reduction) while superior strength-to-emission ratios are maintained.
- The methodology can be adapted for regions with similar industries by product availability, particularly relevant for rapidly developing economies, where cement demand is projected to increase 30–45% by 2030.

The mechanistic understanding we developed—linking elemental ratios, phase development, and performance—provides a fundamental framework for future optimization of sustainable cementitious systems globally. This approach directly addresses construction industry concerns regarding the balance between environmental benefits and mechanical performance, offering a scientifically validated pathway toward next-generation construction materials.

## Conclusions

This research demonstrates that strategic incorporation of regional industrial by-products can transform conventional cement systems, yield exceptional performance enhancements, while dramatically reducing environmental impact. Through systematic investigation of Mae Moh power plant fly ash and Taisei Thailand GGBFS, substantial benefits across multiple performance parameters have been achieved.

Systematic laboratory testing revealed that optimized SCM combinations enhanced rheological properties by 26% compared to conventional cement while maintaining superior strength development. The combination of 40% GGBFS with 20% fly ash achieved 93.5 MPa compressive strength at 90 days—exceeding conventional cement's 91.0 MPa—while simultaneously reducing drying shrinkage by 35% and maintaining comparable permeability characteristics. These results address critical durability concerns in cement-based materials while demonstrating enhanced performance capabilities.

The environmental benefits represent the most compelling aspect of this research. Substituting 40% cement with GGBFS reduced carbon emissions by 64% (from 402.62 to 145.0 kg-$CO_2$/$m^3$), while the combination of 40% GGBFS with 20% fly ash further decreased emissions by 72% (to 113.1 kg-$CO_2$/$m^3$). Most remarkably, complete cement replacement using GGBFS with suitable activators achieved 90% $CO_2$ emission reduction (to 40.3 kg-$CO_2$/$m^3$) while maintaining high mechanical performance (65.0 MPa at 90 days), establishing new benchmarks for sustainable construction materials.

Microstructural analysis identified the mechanisms underlying these improvements: enhanced formation of C-S-H and C-A-S-H phases through efficient pozzolanic reactions and refinement of the cementitious matrix. The systematic reduction in Portlandite content from 15.2 to 1.8% confirmed more effective calcium utilization. The development of the Calcium Utilization Efficiency (CUE) parameter represents a fundamental advancement in cement evaluation, demonstrating remarkable improvement from 63% in conventional systems to 94% in optimized formulations. This metric provides a direct correlation between chemical efficiency and mechanical performance, offering predictive capabilities for sustainable cement design.

This approach provides a framework for utilizing approximately 2.1 million tonnes of industrial by-products produced annually in northern Thailand, simultaneously addressing waste management challenges while creating economically viable alternatives for the construction industry. The research offers particular value for regions with abundant industrial by-products and establishes a replicable model for sustainable material innovation globally.

Practical implementation requires attention to several critical factors: development of standardized quality control protocols ensuring consistent material properties across varying by-product sources, modification of existing production facilities to accommodate multiple supplementary materials with proper activation and updating of regulatory frameworks and construction standards to incorporate these innovative systems.

Future research should focus on four critical areas: long-term durability assessment under varied environmental conditions (particularly carbonation, chloride penetration, and sulfate resistance), development of simplified yet robust quality control methodologies for large-scale production, investigation of more economical activator systems, and optimization of mix designs for specific applications with varying performance requirements.

This research fundamentally challenges conventional cement industry paradigms by proving that environmental sustainability and performance excellence are not mutually exclusive. The findings provide a scientifically validated framework for dramatically reducing the environmental footprint of cement production while enhancing performance, representing a significant advancement toward environmentally responsible construction materials that maintain or exceed conventional performance standards. Through collaboration between researchers, industry stakeholders, and regulatory bodies, these sustainable cement systems can accelerate global alignment with sustainability targets for the construction sector, contributing to urgent decarbonization goals while meeting growing infrastructure demands.

## Data availability

The datasets used and/or analysed during the current study are available from the corresponding author on reasonable request.

Received: 10 March 2025; Accepted: 20 August 2025
Published online: 26 August 2025

## References

1. Mahasenan, N., Smith, S. & Humphreys, K. K., The Cement Industry and Global Climate Change: Current and Potential Future Cement Industry CO2 Emissions, In *Greenhouse Gas Control Technologies – 6th International Conference*, J. Gale and Y. Kaya, Editors. Pergamon: Oxford. pp. 995–1000. (2003).
2. Nguyen, K. T. et al. Theoretical and experimental study on mechanical properties and flexural strength of fly ash-geopolymer concrete. *Constr. Build. Mater.* **106**, 65–77 (2016).
3. Fayomi, G. U. et al. Perspectives on environmental CO2 emission and energy factor in cement industry. *IOP Conf. Series: Earth Environ. Sci.* **331** (1), 012035–p (2019).
4. Van den Heede, P. & De Belie, N. Environmental impact and life cycle assessment (LCA) of traditional and 'green' concretes: literature review and theoretical calculations. *Cem. Concr. Compos.* **34** (4), 431–442 (2012).
5. Schneider, M. et al. Sustainable cement production—present and future. *Cem. Concr. Res.* **41** (7), 642–650 (2011).
6. CEMBUREAU, *Activity Report*. : Brussels. (2017).
7. Wattanachai, P. et al. Development of non-OPC binder using fly Ash, limestone powder, gibbsite powder, and biomass Ash for workability, strength, and CO2 capture. *Sci. Rep.* **15** (1), 11098 (2025).
8. Cross, D., Stephens, J. & Vollmer, J. *Structural Applications of 100% Fly Ash Concrete.* (2005).
9. Hemmings, R. T. & Berry, E. E. *On the Glass in Coal Fly Ashes: Recent Advances.* MRS Proceedings, 113: p. 3. (1987).
10. Qian, J., Lachowski, E. & Glasser, F. *Microstructure and Chemical Variation in Class F Fly Ash Glass.* MRS Proceedings, 113. (2011).
11. Brindle, J. H. & McCarthy, M. J. Chemical constraints on fly Ash glass compositions. *Energy Fuels*. **20** (6), 2580–2585 (2006).
12. Ward, C. & French, D. Determination of glass content and Estimation of glass composition in fly Ash using quantitative X-ray diffractometry. *Fuel* **85**, 2268–2277 (2006).
13. Cohen, M. D. Theories of expansion in sulfoaluminate - type expansive cements: schools of thought. *Cem. Concr. Res.* **13** (6), 809–818 (1983).
14. Naqi, A. & Jang, J. G. Recent progress in green cement technology utilizing Low-Carbon emission fuels and Raw materials: A review. *Sustainability* **11**, 537 (2019).
15. Bhatt, A. et al. Physical, chemical, and geotechnical properties of coal fly ash: A global review. *Case Stud. Constr. Mater.* **11**, e00263 (2019).
16. Garcia-Lodeiro, I. et al. Hydration of hybrid alkaline cement containing a very large proportion of fly ash: A descriptive model. *Materials* **9** (7), 605 (2016).
17. Aydin, E. & Arel, H. Ş. Characterization of high-volume fly-ash cement pastes for sustainable construction applications. *Constr. Build. Mater.* **157**, 96–107 (2017).
18. Juenger, M. et al. *Supplementary Cementitious Materials for Concrete: Characterization Needs.* MRS Proceedings, 1488. (2012).
19. Elyasigorji, F. et al. Comprehensive review of direct and indirect pozzolanic reactivity testing methods. *Buildings* **13** (11), 2789 (2023).
20. Wilson, W. et al. The micromechanical signature of high-volume natural Pozzolan concrete by combined statistical nanoindentation and SEM-EDS analyses. *Cem. Concr. Res.* **91**, 1–12 (2017).
21. Dadsetan, S. & Bai, J. Mechanical and microstructural properties of self-compacting concrete blended with metakaolin, ground granulated blast-furnace slag and fly Ash. *Constr. Build. Mater.* **146**, 658–667 (2017).
22. Tiao, W. et al. Experimental investigation of pozzolanic reaction and curing temperature-dependence of low-calcium fly Ash in cement system and Ca-Si-Al element distribution of fly Ash-blended cement paste. *Constr. Build. Mater.*, 267. (2020).
23. De Weerdt, K. et al. Hydration mechanisms of ternary Portland cements containing limestone powder and fly Ash. *Cem. Concr. Res.* **41** (3), 279–291 (2011).
24. Ogino, M., Miyahara, S., Okanoto, R., Owaki, E. & Nakamura, E. Durability and Applications of Environmental-Friendly Concrete without Portland Cement. International Symposium on Concrete and Structures for Next Generation, Ikeda & Otsuki Symposium. (2016).
25. Tognonvi, M. et al. Reactivity of recycled glass powder in a cementitious medium. *New. J. Glass Ceram.* **10**, 29–44 (2020).
26. International, A. ASTM C109 / C109M-20a standard test method for compressive strength of hydraulic cement mortars (Using 2-in. Or [50-mm] Cube Specimens). : West Conshohocken. (2020).
27. International, A. ASTM C1437-15 Standard Test Method for Flow of Hydraulic Cement Mortar (West Conshohocken, 2015).
28. Aranyasen, S., Srinavin, K., Aksorn, P. & Kusonkhum, W. Comparison of carbon dioxide emissions (CO2-e) produced between ordinary concrete production and geopolymer concrete for environmentally friendly construction industry by using life cycle assessment methods. *KKU Res. J.*, **21**(4). (2021).
29. Association, M. P. Embodied CO2e of UK Cement, Additions and Cementitious Material (MPA Cement, 2019).

30. Scrivener, K., Snellings, R. & Lothenbach, B. *A Practical Guide to Microstructural Analysis of Cementitious Materials*. (2015).
31. Taylor, H. F. W. *Cement Chemistry*. 2nd edition. London: Thomas Telford Publishing. (1997).
32. Lothenbach, B., Durdziński, P. & De Weerdt, K. *Thermogravimetric analysis*. pp. 177–212. (2015).
33. Suwan, C. and Somjai, T., Comparative Greenhouse Gas Evaluation of House Construction: A Conventional House versus an Interlocking Block House. (The Journal of King Mongkut's University of Technology North Bangkok); Vol 30,No 4 (2020).
34. Richardson, I. G. The calcium silicate hydrates. *Cem. Concr. Res.* **38**, 137–158 (2008).
35. International, A. *ASTM C311/C311M-18, Standard Test Methods for Sampling and Testing Fly Ash or Natural Pozzolans for Use in Portland-Cement Concrete* (West Conshohocken, 2018).
36. International, A. *ASTM C618-19, Standard Specification for Coal Fly Ash and Raw or Calcined Natural Pozzolan for Use in Concrete* (West Conshohocken, 2019).
37. Oner, A. & Akyuz, S. An experimental study on optimum usage of GGBS for the compressive strength of concrete. *Cem. Concr. Compos.* **29**, 505–514 (2007).
38. Rashad, A. M. A brief on high-volume class F fly Ash as cement replacement – A guide for civil engineer. *Int. J. Sustainable Built Environ.* **4** (2), 278–306 (2015).

## Acknowledgements

The authors gratefully acknowledge the financial support of Chiang Mai University to the author to do the practical work reported in this paper.

## Author contributions

Pitiwat Wattanachai (PW), Kedsarin Pimraksa (KP), Sattaya Chaiwithee (SC), Thaloengsak Keereemasthong (TK), Kittiphat Kochchapong (KK)PW, KP, SC: Conceptualization PW, KP, SC, TK, KK: Methodology PW, SC, Tk, KK: Writing-review and editing PW, KP: Supervision PW, KP, SC, TK, KK: Formal analysis SC, TK, KK: Investigation PW, KP: Resource PW, SC: Writing-original KP: Validation PW: Project administration.

## Funding

The authors gratefully acknowledge the financial support of Chiang Mai University, which was provided to Pitiwat Wattanachai.

## Declarations

## Competing interests

The authors declare no competing interests.

## Additional information

**Correspondence** and requests for materials should be addressed to P.W.

**Reprints and permissions information** is available at www.nature.com/reprints.

**Publisher's note** Springer Nature remains neutral with regard to jurisdictional claims in published maps and institutional affiliations.